

Site-Specific Incorporation of 3-Nitrotyrosine as a Probe of pK_a Perturbation of Redox-Active Tyrosines in Ribonucleotide Reductase

Kenichi Yokoyama,[†] Ulla Uhlin,[§] and JoAnne Stubbe^{*,†,‡}

Departments of Chemistry and Biology, Massachusetts Institute of Technology, 77 Massachusetts Avenue, Cambridge, Massachusetts 02139-4307, and Department of Molecular Biology, Swedish University of Agricultural Science, Uppsala Biomedical Center, Box 590, SE-75124 Uppsala, Sweden

Received February 6, 2010; E-mail: stubbe@mit.edu

Abstract: *E. coli* ribonucleotide reductase catalyzes the reduction of nucleoside 5'-diphosphates into 2'-deoxynucleotides and is composed of two subunits: $\alpha 2$ and $\beta 2$. During turnover, a stable tyrosyl radical (Y^\bullet) at Y_{122} - $\beta 2$ reversibly oxidizes C_{439} in the active site of $\alpha 2$. This radical propagation step is proposed to occur over 35 Å, to use specific redox-active tyrosines (Y_{122} and Y_{356} in $\beta 2$, Y_{731} and Y_{730} in $\alpha 2$), and to involve proton-coupled electron transfer (PCET). 3-Nitrotyrosine (NO_2Y , pK_a 7.1) has been incorporated in place of Y_{122} , Y_{731} , and Y_{730} to probe how the protein environment perturbs each pK_a in the presence of the second subunit, substrate (S), and allosteric effector (E). The activity of each mutant is $<4 \times 10^{-3}$ that of the wild-type (wt) subunit. The $[NO_2Y_{730}]$ - $\alpha 2$ and $[NO_2Y_{731}]$ - $\alpha 2$ each exhibit a pK_a of 7.8–8.0 with E and E/ $\beta 2$. The pK_a of $[NO_2Y_{730}]$ - $\alpha 2$ is elevated to 8.2–8.3 in the S/E/ $\beta 2$ complex, whereas no further perturbation is observed for $[NO_2Y_{731}]$ - $\alpha 2$. Mutations in pathway residues adjacent to the NO_2Y that disrupt H-bonding minimally perturb its pK_a . The pK_a of NO_2Y_{122} - $\beta 2$ alone or with $\alpha 2$ /S/E is >9.6 . X-ray crystal structures have been obtained for all $[NO_2Y]$ - $\alpha 2$ mutants (2.1–3.1 Å resolution), which show minimal structural perturbation compared to wt- $\alpha 2$. Together with the pK_a of the previously reported NO_2Y_{356} - $\beta 2$ (7.5 in the $\alpha 2$ /S/E complex; Yee, C. et al. *Biochemistry* **2003**, *42*, 14541–14552), these studies provide a picture of the protein environment of the ground state at each Y in the PCET pathway, and are the starting point for understanding differences in PCET mechanisms at each residue in the pathway.

Introduction

Class Ia ribonucleotide reductases (RNRs) play a crucial role in DNA replication and repair, catalyzing the reduction of nucleoside 5'-diphosphates (NDPs) to 2'-deoxynucleoside 5'-diphosphates (dNDPs).^{1–3} *E. coli* RNR consists of two homodimeric subunits: $\alpha 2$ and $\beta 2$. $\alpha 2$ houses the binding sites for substrates (S) and effectors (E), where S is UDP, CDP, ADP, or GDP and E is ATP, dATP, TTP, or dGTP that control the specificity and rate of nucleotide reduction. $\beta 2$ harbors the radical initiator, a diferric tyrosyl radical (Y_{122}^\bullet) cofactor, which reversibly and transiently oxidizes C_{439} in the active site of $\alpha 2$. This thyl radical initiates nucleotide reduction. The crystal structure of *E. coli* $\alpha 2$ ^{4,5} and of $\beta 2$ ^{6,7} have been independently solved. A crystal structure of the class Ib RNR from *Salmonella*

typhimurium containing both subunits has also been reported at 4.5 Å resolution and may be indicative of an intermediate in the formation of the active RNR complex that has remained elusive.⁸ A docking model by Uhlin and Eklund using the structures of $\alpha 2$ and $\beta 2$ has been generated on the basis of shape complementarity, in which the stable Y_{122}^\bullet in $\beta 2$ is >35 Å from the C_{439} in $\alpha 2$.⁴ This distance is too large for electron tunneling, given the enzyme's turnover number of $1–10 \text{ s}^{-1}$.^{9–11} These observations led to the proposal that the radical propagation proceeds by a hopping mechanism through conserved aromatic amino acid residues located in $\alpha 2$ and $\beta 2$ (Figure 1).^{4,12–15} This paper reports the site-specific incorporation of the unnatural amino acid 3-nitrotyrosine (NO_2Y) in place of Y_{122} in $\beta 2$ and

[†] Department of Chemistry, Massachusetts Institute of Technology.

[‡] Department of Biology, Massachusetts Institute of Technology.

[§] Swedish University of Agricultural Science.

- (1) Stubbe, J.; van der Donk, W. A. *Chem. Rev.* **1998**, *98*, 705–762.
- (2) Jordan, A.; Reichard, P. *Annu. Rev. Biochem.* **1998**, *67*, 71–98.
- (3) Nordlund, P.; Reichard, P. *Annu. Rev. Biochem.* **2006**, *75*, 681–706.
- (4) Uhlin, U.; Eklund, H. *Nature* **1994**, *370*, 533–539.
- (5) Eriksson, M.; Uhlin, U.; Ramaswamy, S.; Ekberg, M.; Regnstrom, K.; Sjöberg, B.-M.; Eklund, H. *Structure* **1997**, *5*, 1077–1092.
- (6) Nordlund, P.; Sjöberg, B.-M.; Eklund, H. *Nature* **1990**, *345*, 593–598.
- (7) Högbom, M.; Galander, M.; Andersson, M.; Kolberg, M.; Hofbauer, W.; Lassmann, G.; Nordlund, P.; Lendzian, P. *Proc. Natl. Acad. Sci. U.S.A.* **2003**, *100*, 3209–3214.

- (8) Uppsten, M.; Farnegardh, M.; Domkin, V.; Uhlin, U. *J. Mol. Biol.* **2006**, *359*, 365–377.

- (9) Marcus, R. A.; Sutin, N. *Biochim. Biophys. Acta* **1985**, *811*, 265–322.
- (10) Moser, C. C.; Keske, J. M.; Warncke, K.; Farid, R. S.; Dutton, P. L. *Nature* **1992**, *355*, 796–802.
- (11) Gray, H. B.; Winkler, J. R. *Annu. Rev. Biochem.* **1996**, *65*, 537–561.
- (12) Siegbahn, P. E. M.; Eriksson, L.; Himo, F.; Pavlov, M. *J. Phys. Chem. B* **1998**, *102*, 10622–10629.
- (13) Ekberg, M.; Sahlin, M.; Eriksson, M.; Sjöberg, B.-M. *J. Biol. Chem.* **1996**, *271*, 20655–20659.
- (14) Reece, S. Y.; Hodgkiss, J. M.; Stubbe, J.; Nocera, D. G. *Philos. Trans. R. Soc., B* **2006**, *361*, 1351–1364.
- (15) Stubbe, J.; Nocera, D.; Yee, C. S.; Chang, M. C. Y. *Chem. Rev.* **2003**, *103*, 2167–2201.

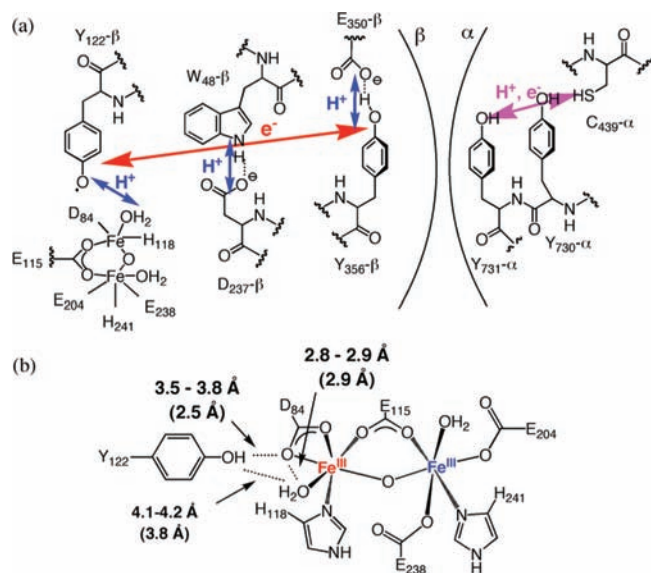


Figure 1. Tyrosines responsible for the PCET in *E. coli* class I RNR. (a) Proposed PCET pathway. Red and blue arrows indicate orthogonal transfer of the electron and proton, respectively. The purple arrow indicates co-linear movement of the electron and proton. (b) Structure of the tyrosine-diferrous cluster.⁶ Distances in parentheses are those of the Mn₂-β₂.^{7,3}

Y₇₃₁ and Y₇₃₀ in α₂. The studies with these constructs reveal that NO₂Y is an excellent probe of how the protein environment modulates the pK_a of the phenol, which is important for thinking about the different mechanisms of proton-coupled electron transfer (PCET) between Y₁₂₂ and C₄₃₉.

Evidence for the radical propagation pathway shown in Figure 1 has come from a number of different experiments. Initially, site-directed mutagenesis of each of the conserved aromatic residues on the proposed pathway demonstrated that each is necessary for RNR activity.^{13,16,17} However, the inactivity of these mutants precluded further mechanistic investigation. Strong support for the redox role of Y₃₅₆ in β₂ was obtained by site-specific incorporation of a variety of tyrosine analogues in place of this residue by the use of expressed protein ligation (EPL) methodology. β₂ with 3,4-dihydroxyphenylalanine (DOPA) at 356 generated DOPA radical (DOPA•) in a kinetically competent fashion when incubated with α₂/S or α₂/S/E.¹⁸ A series of fluorotyrosine analogues (F_nY, n = 2, 3, 4) incorporated into this position allowed modulation of the residue's reduction potential and pK_a,^{19,20} both of which play an important role in PCET.^{14,15} Comparison of the activities of Y₃₅₆F_nY-β₂s relative to wild-type (wt)-β₂ as a function of pH showed that nucleotide reduction could be modulated by reduction potential.¹⁹ In addition, studies with 3,5-F₂Y-β₂ showed no obligate coupling between the electron and proton transfer at this residue during radical transport.²¹ These results suggest that PCET through Y₃₅₆ involves orthogonal (bidirectional) PCET in which electron and proton are transferred to different acceptors (Figure 1).^{14,15}

Crystallographic data of *E. coli* α₂ suggests that PCET within this subunit may occur by a mechanism distinct from that proposed for 356 in β. Y₇₃₁, Y₇₃₀, and C₄₃₉-α₂ are within H-bonding distance of one another, and the unusual orientation of Y₇₃₁ and Y₇₃₀ relative to one another (Figure 1) suggests that π-π stacking may occur. This structural insight, in conjunction with theory, has resulted in the proposal of co-linear PCET within α₂ in which an electron and a proton are transferred between the same donor/acceptor pair (Figure 1).^{4,12,14,15,22} Radical propagation in α₂ has also been investigated by site-specific incorporation of 3-aminotyrosine (NH₂Y) in place of Y₇₃₁ and Y₇₃₀ in α by the orthogonal aminoacyl tRNA synthetase (RS)/tRNA method.²³ The NH₂Y residues of [NH₂Y₇₃₁]-α₂ and [NH₂Y₇₃₀]-α₂ in the presence of β₂/S and β₂/S/E are oxidized to an aminotyrosyl radical (NH₂Y•) in a kinetically competent fashion, suggesting that these Y residues are redox-active. Recent studies, in which NH₂Y was incorporated "off-pathway",²⁴ in conjunction with the [NH₂Y₇₃₁]-α₂ and [NH₂Y₇₃₀]-α₂ studies suggest that radical propagation occurs by a specific pathway.

Several additional results support the proposal of a co-linear PCET (also called hydrogen atom transfer, HAT) mechanism within α. The first is our studies with a photoreactive-Y₃₅₆R2C19mer peptide complexed to α. This 20mer peptide, identical to the 20 C-terminal amino acid residues of β including Y₃₅₆, contains an appended photo-oxidant at its N-terminus. It forms a complex with α₂ and makes deoxynucleotides subsequent to light-mediated oxidation of Y₃₅₆, thus acting as a competent surrogate for the entire β₂.^{25,26} The results with the α mutant Y₇₃₀F and different photooxidants supports the proton-dependent hopping mechanism.^{26,27} The second is the observation that [NH₂Y₇₃₁]- and [NH₂Y₇₃₀]-α₂ and, more recently, [NH₂Y₃₅₆]-β₂ (E. C. Minnihan, and J. Stubbe, unpublished results) are active in nucleotide reduction. An energetic analysis of the possible mechanisms of oxidation of C₄₃₉-α₂ by NH₂Y₇₃₀-α₂ supports a hydrogen atom transfer mechanism.²³

The experimental data obtained thus far suggest that different mechanisms of PCET occur at different residues within the pathway, which in part is a reflection of differences in the protein environment at each site.^{4,6,14} In order to think about the mechanism of PCET at each site (Figure 1), a knowledge of the H-bonding interactions and pK_a perturbations of each Y within the pathway is necessary.^{14,15} Given the number of enzymes that utilize a transient Y• in conversion of their substrate to product,^{1,28} development of a method to study the pK_a of a single Y in a protein with many Ys is of general interest.

As a demonstration of its utility, we previously introduced NO₂Y in place of Y₃₅₆ in β₂ and showed that its pK_a was perturbed 0.2 pH units in the presence of α₂/ADP/dGTP, relative to the pK_a of *N*-acetyl-3-nitrotyrosine amide in aqueous solu-

- (16) Climent, I.; Sjöberg, B.-M.; Huang, C. Y. *Biochemistry* **1992**, *31*, 4801–4807.
 (17) Ekberg, M.; Birgander, P.; Sjöberg, B.-M. *J. Bacteriol.* **2003**, *185*, 1167–1173.
 (18) Seyedsayamdost, M. R.; Stubbe, J. *J. Am. Chem. Soc.* **2006**, *128*, 2522–2523.
 (19) Seyedsayamdost, M. R.; Yee, C. S.; Reece, S. Y.; Nocera, D. G.; Stubbe, J. *J. Am. Chem. Soc.* **2006**, *128*, 1562–1568.
 (20) Seyedsayamdost, M. R.; Reece, S. Y.; Nocera, D. G.; Stubbe, J. *J. Am. Chem. Soc.* **2006**, *128*, 1569–1579.
 (21) Yee, C. S.; Chang, M. C.; Ge, J.; Nocera, D. G.; Stubbe, J. *J. Am. Chem. Soc.* **2003**, *125*, 10506–10507.

- (22) DiLabio, G. A.; Johnson, E. R. *J. Am. Chem. Soc.* **2007**, *129*, 6199–6203.
 (23) Seyedsayamdost, M. R.; Xie, J.; Chan, C. T.; Schultz, P. G.; Stubbe, J. *J. Am. Chem. Soc.* **2007**, *129*, 15060–15071.
 (24) Minnihan, E. C.; Seyedsayamdost, M. R.; Stubbe, J. *Biochemistry* **2009**, *48*, 12125–12132.
 (25) Chang, M. C.; Yee, C. S.; Stubbe, J.; Nocera, D. G. *Proc. Natl. Acad. Sci. U.S.A.* **2004**, *101*, 6882–6887.
 (26) Reece, S. Y.; Seyedsayamdost, M. R.; Stubbe, J.; Nocera, D. G. *J. Am. Chem. Soc.* **2007**, *129*, 8500–8509.
 (27) Reece, S. Y.; Seyedsayamdost, M. R.; Stubbe, J.; Nocera, D. G. *J. Am. Chem. Soc.* **2007**, *129*, 13828–13830.
 (28) Pesavento, R. P.; van der Donk, W. A. *Adv. Protein Chem.* **2001**, *58*, 317–385.

tion.²⁹ We proposed that NO₂Y would be an excellent probe for a several reasons, albeit with some caveats. First, its pK_a of 7.1 is in the middle of the pH range where most proteins, including RNR, are stable. Second, the absorption maximum for its phenol and phenolate at 360 and 424 nm, respectively, possess moderately large extinction coefficients and absorption features removed from the protein envelope, facilitating titrations as a function of pH. Finally, in the case of probing redox-active Ys, NO₂Y is harder to oxidize than Y by 210 mV at pH 7. Thus, in the case of RNR, its incorporation would result in protein incapable of nucleotide reduction due to a block in the pathway, while retaining sensitivity to environmental changes associated with S and E binding. A drawback associated with the NO₂Y probe is that it can form an intramolecular H-bond with the OH of the phenol. Its strength will depend on the orientation of the NO₂ group relative to the plane of the phenyl ring and the hydrophobicity of its environment. Studies of *o*- and *p*-substituted nitrophenols (Table S1 in Supporting Information) reveal that the *o*-substituted phenols have elevated pK_as relative to the *p*-substituted phenols with the extent of pK_a elevation being dependent on solvent.^{30–34} The ability to form intramolecular H-bonds will undoubtedly perturb reporting on intermolecular H-bonding within the protein. However, if the orientation of the NO₂ group remains similar with different mutants, relative pK_as will be informative.

In this work, we have used the NO₂Y-RS/tRNA pair, recently evolved by the Chin and Mehl groups,³⁵ to successfully incorporate NO₂Y in place of Y₇₃₁ and Y₇₃₀ of α2 and Y₁₂₂ of β2. The EPL method, used to incorporate NO₂Y in place of Y₃₅₆, is not applicable for Y₇₃₁ and Y₇₃₀ because of the large size of the protein and the buried nature of the backbone of these residues. The pK_a of each of these NO₂Ys (Figure 1) has been determined in the presence of a single protein subunit and in the α2β2/E and α2β2/E/S complexes. Together with the previously determined pK_as of NO₂Y at 356-β2,²⁹ the data suggest distinct, position-dependent pK_as with minimal perturbations for the three Ys (730, 731-α2, and 356-β2) that form transient radicals, compared to the large perturbation at the stable Y• site, Y₁₂₂. In addition, substrate binding perturbs the pK_a of NO₂Y only at 730. Additional mutations adjacent to the NO₂Y substitution were introduced at positions 731, 730, and 439 in α2, to investigate the effect of the H-bonding interactions (Figure 1) on the pK_a. Minimal effects were observed. Finally, the crystal structures for all the [NO₂Y]-α2 have been obtained to 2.1–3.1 Å resolution and show minimal structural perturbations relative to the wt-α2 crystallized under identical conditions. The NO₂ group is planar with the phenol ring of residue 730 and shows two orientations (planar and perpendicular to the phenol ring) in residue 731. The results of NO₂Y incorporation in these three positions provide the foundation for thinking about differences in mechanism of PCET at different residues in the

pathway. The results further demonstrate that NO₂Y is a sensitive reporter on protein environment.

Materials and Methods

Luria–Bertani (LB) medium, BactoAgar, and 100 mm Petri dish plates were obtained from Becton-Dickinson. NO₂Y, M9 salts, ampicillin (Amp), L-arabinose (L-Ara), chloramphenicol (Cm), all amino acids, ATP, 2'-deoxyguanine 5'-triphosphate (dGTP), cytidine 5'-diphosphate (CDP), adenine 5'-diphosphate (ADP), NADPH, ethylenediamine tetraacetic acid (EDTA), Bradford Reagent, Sephadex G-25, phenylmethanesulfonyl fluoride (PMSF), and streptomycin sulfate were purchased from Sigma-Aldrich. Isopropyl-β-D-thiogalactopyranoside (IPTG), dithiothreitol (DTT), *DpnI*, and T4 DNA ligase were from Promega. pBAD/*Myc*-His A, *E. coli* DH5α and TOP10 competent cells, pCR2.1-TOPO, bacterial alkaline phosphatase, and oligonucleotides were from Invitrogen. Calf-intestine alkaline phosphatase (CIAP, 20 U/μL) was from Roche. *NcoI*, *XhoI*, *SalI*, *BglII*, *NdeI*, and *PstI* were from New England Biolabs. The purification of *E. coli* thioredoxin³⁶ (TR, 40 units/mg), *E. coli* thioredoxin reductase³⁷ (TRR, 1400 units/mg), and wild-type (wt)-β2³⁸ (6200–7200 nmol/min/mg, 1–1.2 radicals per β2) and wt-α2³⁹ (2300–2600 nmol/min/mg) have previously been described. The concentrations of α2 and [NO₂Y]-α2s were determined using ε_{280 nm} = 189 mM⁻¹ cm⁻¹.⁴⁰ The concentrations of β2 and [NO₂Y]₁₂₂-β2 were determined using ε_{280 nm} = 131 mM⁻¹ cm⁻¹.⁴⁰ The concentrations of apo-[NO₂Y]₁₂₂-β2 were determined using ε_{280 nm} = 120 mM⁻¹ cm⁻¹.⁴¹ Glycerol minimal media leucine (GMMML)⁴² contains final concentrations of 1% (v/v) glycerol, 1 × M9 salts, 0.05% (w/v) NaCl, 1 mM MgSO₄, 0.1 mM CaCl₂, and 0.3 mM L-leucine. RNR assay buffer consists of 50 mM HEPES, 15 mM MgSO₄, 1 mM EDTA, pH 7.6. UV-vis absorption spectra and the spectrophotometric assays were carried out using a Cary 3 UV-vis spectrophotometer (Varian, Walnut Creek, CA). The Ultramark EX Microplate Imaging System (BioRad) was used to determine A_{280 nm} for protein, A_{340 nm} for ferric cluster and NO₂Y phenol, A_{490 nm} for NO₂Y phenolate of fractions after column chromatography. All DNA sequences were confirmed by the MIT Biopolymers Laboratory. PCR was carried out using PfuUltraII polymerase (Stratagene) according to the manufacturer's protocol. The annealing temperature and number of cycles varied are described individually. For site-directed mutagenesis, PCR was performed for 18 cycles with annealing temperature of 55 °C, followed by *DpnI* digestion of methylated template plasmid. The primers used for PCR are summarized in Table S2 in Supporting Information. pSUP-3NT/8³⁵ was kindly supplied by Dr. J. W. Chin (Medical Research Council Laboratory of Molecular Biology, Cambridge, U.K.) and Dr. R. A. Mehl's lab (Franklin & Marshall College, Lancaster), and pEVOL⁴³ was a kind gift of Dr. P. G. Schultz (The Scripps Research Institute, San Diego).

Construction of pBAD-*nrdA*-Y₇₃₀Z and pBAD-*nrdA*-Y₇₃₁Z. *nrdA* was amplified by PCR using pMJ1-*nrdA*⁴⁴ as a template with primers, *nrdA*-f and *nrdA*-r (Table S2 in Supporting Information) that harbor *NcoI* and *XhoI* restriction sites, respectively. Introduction of the *NcoI* site changed the first base of the second codon, A to G, which mutated the second amino acid, Asn to Asp. PCR was

(29) Yee, C. S.; Seyedsayamdost, M. R.; Chang, M. C.; Nocera, D. G.; Stubbe, J. *Biochemistry* **2003**, *42*, 14541–14552.

(30) Rived, F.; Rosés, M.; Bosch, E. *Anal. Chim. Acta* **1998**, *374*, 309–324.

(31) Maran, F.; Celadon, M. G.; Severin, E.; Vianello, E. *J. Am. Chem. Soc.* **1991**, *113*, 9320–9329.

(32) Izutsu, K. *Acid-Base Dissociation Constants in Dipolar Aprotic Solvents*; Blackwell Scientific Publications: Oxford, 1990.

(33) Bosch, E.; Roses, M. *Talanta* **1989**, *36*, 627–632.

(34) Bosch, E.; Rafols, M.; Roses, M. *Talanta* **1989**, *36*, 1227–1231.

(35) Neumann, H.; Hazen, J. L.; Weinstein, J.; Mehl, R. A.; Chin, J. W. *J. Am. Chem. Soc.* **2008**, *130*, 4028–4033.

(36) Chivers, P. T.; Prehoda, K. E.; Volkman, B. F.; Kim, B. M.; Markley, J. L.; Raines, R. T. *Biochemistry* **1997**, *36*, 14985–14991.

(37) Pigiet, V. P.; Conley, R. R. *J. Biol. Chem.* **1977**, *252*, 6367–6372.

(38) Salowe, S. P.; Stubbe, J. *J. Bacteriol.* **1986**, *165*, 363–366.

(39) Salowe, S. P.; Ator, M. A.; Stubbe, J. *Biochemistry* **1987**, *26*, 3408–3416.

(40) Thelander, L. *J. Biol. Chem.* **1973**, *248*, 4591–4601.

(41) Atkin, C. L.; Thelander, L.; Reichard, P.; Lang, G. *J. Biol. Chem.* **1973**, *248*, 7464–7472.

(42) Wang, J.; Brock, A.; Herberich, B.; Schultz, P. G. *Science* **2001**, *292*, 498–500.

(43) Young, T. S.; Ahmad, I.; Yin, J. A.; Schultz, P. G. *J. Mol. Biol.* **2010**, *395*, 361–374.

(44) Mao, S. S.; Johnston, M. I.; Bollinger, J. M.; Stubbe, J. *Proc. Natl. Acad. Sci. U.S.A.* **1989**, *86*, 1485–1489.

carried out as described above for 40 cycles with an annealing temperature of 58 °C. The product was digested with *NcoI* and *XhoI* and subcloned into pBAD/*MycHis-A* to give pBAD-*nrdA*. The TAG codon (Z) was inserted at 730 or 731 using primers Y730Z-f and Y730Z-r for 730, and Y731Z-f and Y731Z-r for 731 (Table S2 in Supporting Information). The mutation accompanied by *NcoI* site introduction in the first PCR was repaired using primers *nrdA*-repair-f and *nrdA*-repair-r (Table S2) to give pBAD-*nrdA*-Y₇₃₀Z and pBAD-*nrdA*-Y₇₃₁Z.

Construction of pEVOL-NO₂Y. pEVOL⁴³ carries two copies of an RS gene, one with *SalI* and *BglIII* sites and the other with *NdeI* and *PstI* sites in the upstream and downstream regions of the gene, respectively. *SalI* and *BglIII* sites were introduced into the 3-nitrotyrosine RS (NO₂Y-RS) gene by PCR using pSUP-3NT/8³⁵ as a template and primers RS-f and RS-r (Table S2 in Supporting Information). PCR was carried out for 30 cycles with an annealing temperature of 55 °C. Adenine was then added to the 3'-terminus of the PCR product for TA ligation by incubation with GO-Taq Hot start polymerase (Promega) in the presence of 0.2 mM dATP at 72 °C for 30 min. The product was ligated with pCR2.1-TOPO (Invitrogen) following the manufacturer's protocol. The resulting plasmid was first digested with *BglIII*, and a 3.9 kb DNA fragment containing NO₂Y-RS gene was isolated and further digested with *SalI*. The second NO₂Y-RS gene with *NdeI* and *PstI* sites was prepared by digesting pSUP-3NT/8 with *NdeI* and *PstI*. The two NO₂Y-RS gene fragments were sequentially introduced into pEVOL. Initially, the NO₂Y-RS gene flanked by *NdeI/PstI* was ligated into pEVOL. The NO₂Y-RS gene flanked with *BglIII/SalI* was then ligated into the new construct to give pEVOL-NO₂Y.

Expression of [NO₂Y₇₃₀]-α2 and [NO₂Y₇₃₁]-α2. *E. coli* TOP10 was transformed with pSUP-3NT/8³⁵ (Cm) and pBAD-*nrdA*-Y₇₃₀Z and grown overnight on LB agar plates. All growths were carried out in the presence of Cm (25 mg/L) and Amp (100 mg/L). A single colony was picked and grown in LB to saturation (~16 h). Two mL of this solution was diluted into 200 mL of LB in a 500 mL baffled flask and grown at 37 °C until saturation. A portion of this culture (100 mL) was then inoculated into a fermenter containing 10 L of GMML medium (pH 6.8) supplemented with Cm (25 mg/L), Amp (100 mg/L), 17 amino acids (Glu, Gln, Asp, Asn, Lys, Val, Arg, Leu, His, Ile, Ala, Pro, Trp, Gly, Met, Thr, Ser, 0.2 g/L each), D-glucose 0.05% (w/v), Asp 0.25% (w/v), L-Ara 0.1% (w/v), and 1X heavy metal solution. The heavy metal stock solution (1000X) contained the following per liter:⁴⁵ 500 mg of Na₂MoO₄·2H₂O, 250 mg of CoCl₂, 175 mg of CuSO₄·5H₂O, 1 g of MnSO₄·H₂O, 8.75 g of MgSO₄·7H₂O, 1.25 g of ZnSO₄·7H₂O, 1.25 g of FeCl₂·4H₂O, 2.5 g of CaCl₂·2H₂O, and 1 g of H₃BO₃, dissolved in 1 M HCl. NO₂Y (2 mM) was added at the beginning of the culture, and growth was continued for 30 h (OD₆₀₀ = 2.6–2.8) at which time the cells were harvested by centrifugation, frozen in liquid N₂ and stored at –80 °C. Typically, 5–6 g of wet cell paste/L was obtained. Expression of [NO₂Y₇₃₁]-α2 and all double mutants was carried out in an identical fashion using the appropriate pBAD constructs.

Purification of [NO₂Y₇₃₀]-α2 and [NO₂Y₇₃₁]-α2. [NO₂Y]-α2s were typically purified from 60–80 g of cell paste. All purification steps were carried out at 4 °C. The cell paste was resuspended in 5 vol of buffer A (50 mM Tris pH 7.6, 1 mM EDTA, 1 mM PMSF and 5 mM DTT). The cells were lysed by a single passage through a French pressure cell operating at 14 000 psi. After removal of cell debris by centrifugation (20 000g, 20 min, 4 °C), DNA was precipitated by dropwise addition of 0.2 vol of buffer A containing 8% (w/v) streptomycin sulfate. The mixture was stirred for an additional 15 min, and the precipitated DNA was removed by centrifugation (20 000g, 20 min, 4 °C). Solid (NH₄)₂SO₄ (3.9 g per 10 mL of supernatant) was then added over 15 min (66% saturation). The solution was stirred for an additional 20 min, and the precipitated protein was isolated by centrifugation (20 000g, 20 min,

4 °C). The pellet was dissolved in a minimal volume of buffer A and desalted using a Sephadex G-25 column (5 cm × 50 cm, 1 L). The desalted protein was loaded onto DEAE Fast Flow column (7 cm × 14 cm, 500 mL), which had been equilibrated in buffer A. The column was washed with 2 L of buffer A containing 50 mM NaCl followed by a gradient (1 L × 1 L) of 50–500 mM NaCl in buffer A. Fractions (10 mL each) containing [NO₂Y]-α2 were judged by SDS-PAGE and differences of phenolate absorption (A_{490 nm}) at pH 7.6 and 9.0. [NO₂Y]-α2 was typically eluted at 210–250 mM NaCl. Pooled fractions were then directly loaded onto a dATP affinity column⁴⁶ (1.5 cm × 4 cm, 100 mL), which had been equilibrated in buffer A. The column was washed with 10 column volumes of buffer A. [NO₂Y]-α2 was then eluted with buffer B (50 mM Tris pH 7.6, 5% glycerol, 1 mM EDTA, 15 mM MgSO₄, and 5 mM DTT) supplemented with 5 mM ATP and 5 mM DTT. Fractions containing [NO₂Y]-α2, judged by SDS-PAGE, were pooled and concentrated by ultrafiltration (Amicon YM-30, Millipore) and loaded onto Q-sepharose HP (Sigma-Aldrich, 3 × 5 cm, 35 mL), which had been equilibrated in buffer C (50 mM Tris pH 8.0, 5% glycerol, 1 mM EDTA, 15 mM MgSO₄, and 5 mM DTT). The column was washed with buffer C containing 50 mM NaCl and 1 mM ATP. ATP was added to prevent equilibration between the monomer and dimer of α, which results in the protein eluting over a larger volume. The protein was eluted using a gradient (300 mL × 300 mL) of 50–500 mM NaCl in the same buffer. Fractions containing [NO₂Y]-α2 (typically, 160–210 mM NaCl), judged by SDS-PAGE, were then concentrated by ultrafiltration as above and desalted using a Sephadex G-25 column (1.1 cm × 100 cm, 100 mL) equilibrated with buffer B. The resultant protein solution was concentrated to ~90 μM, frozen in liquid N₂, and stored at –80 °C. Typically, 1–3 mg of [NO₂Y]-α2s per gram of wet cell paste was obtained.

Generation and Expression of [NO₂Y₁₂₂]-β2. A TAG codon was introduced by PCR using pBAD-*nrdB*-NS5⁴⁷ as a template and primers Y122Z-f and Y122Z-r (Table S2 in Supporting Information). *NrdB* encoded in pBAD-*nrdB*-NS5 has a StrepII tag (WSHPQFEK) at its N-terminus followed by a 5 amino acid linker (SLGGH). The resulting plasmid, pBAD-*nrdB*-NS5-Y₁₂₂Z (Amp^R), was introduced into *E. coli* TOP10 together with pEVOL-NO₂Y (Cm) and grown overnight on LB agarose plates. All growths were carried out in the presence of Cm (25 mg/L) and Amp (100 mg/L). A single colony was picked and grown in 5 mL of LB to saturation (~16 h). Two mL of this solution was diluted into 200 mL of LB in a 500 mL baffled flask and grown at 37 °C until saturation (~10 h). A portion of this culture (100 mL) was then inoculated into a fermenter containing 10 L of the 17 amino acids supplemented GMML medium described above. NO₂Y (2 mM) was added at the beginning of the culture, and growth was continued for 15 h (OD₆₀₀ = 1.5–1.8) at which point the cells were harvested by centrifugation, frozen in liquid N₂, and stored at –80 °C. Typically, 2–3 g of wet cell paste/L was obtained.

Purification of [NO₂Y₁₂₂]-β2. [NO₂Y₁₂₂]-β2 was purified from 30–40 g wet cell paste. Although the [NO₂Y₁₂₂]-β2 is strep-tagged, the standard protocol³⁸ for β2 purification was used for large-scale preparations because of the poor binding of tagged [NO₂Y₁₂₂]-β2 to *Strep*-Tactin sepharose (IBA, St. Louis, MO). All steps were carried out at 4 °C. The cell paste was resuspended in 5 vol of buffer D (50 mM Tris pH 7.6, 5% glycerol and 0.5 mM PMSF). The cells were lysed by a single passage through a French pressure cell operating at 14 000 psi. Fe^{II}(NH₄)₂(SO₄)₂ and sodium ascorbate (5 mg each per gram of cell paste) were added to the lysate and stirred for 10 min. After removal of cell debris by centrifugation (20 000g, 20 min, 4 °C), DNA was precipitated by dropwise addition of 0.2 volumes of buffer D containing 6% (w/v) streptomycin sulfate. The mixture was stirred for an additional 15 min, and the precipitated DNA was removed by centrifugation (20 000g,

(45) Farrell, I. S.; Toroney, R.; Hazen, J. L.; Mehl, R. A.; Chin, J. W. *Nat. Methods* **2005**, *2*, 377–384.

(46) Berglund, O.; Eckstein, F. *Methods Enzymol.* **1974**, *34*, 253–261.

(47) Hristova, D.; Wu, C. H.; Jiang, W.; Krebs, C.; Stubbe, J. *Biochemistry* **2008**, *47*, 3989–3999.

20 min, 4 °C). Solid (NH₄)₂SO₄ (3.9 g per 10 mL of supernatant) was then added over 15 min (66% saturation). The solution was stirred for an additional 20 min, and the precipitated protein was isolated by centrifugation (20 000g, 20 min, 4 °C). The pellet was dissolved in a minimal volume of buffer D and desalted using a Sephadex G-25 column (5 cm × 50 cm, 1 L). The desalted protein was loaded onto DEAE Fast Flow column (5 cm × 13 cm, 250 mL), which had been equilibrated in buffer D. The column was washed with 1.5 L of buffer D containing 100 mM NaCl followed by a gradient (1 L × 1 L) of 100–500 mM NaCl in buffer D. Fractions containing [NO₂Y₁₂₂]-β2 were judged by SDS–PAGE and A_{340 nm}, the absorption feature of diferric cluster and 3-nitrophenol. [NO₂Y₁₂₂]-β2 typically eluted at 190–220 mM NaCl. The resulting fractions were then diluted 2-fold using buffer D and were loaded onto a Q-sepharose fast flow column (4.5 cm × 10 cm, 150 mL), which had been equilibrated in buffer D. The column was washed with 1.5 L of buffer D containing 150 mM NaCl followed by a gradient (1 L × 1 L) of 150–500 mM NaCl in buffer D. Fractions containing [NO₂Y₁₂₂]-β2 (220–250 mM NaCl), judged by SDS–PAGE, were pooled and concentrated by ultrafiltration (Amicon YM-30, Millipore) to ~500 μM, frozen in liquid N₂, and stored at –80 °C. Typically, 7 mg of [NO₂Y₁₂₂]-β2 per g of wet cell paste was obtained. The iron content was determined by the ferrozine assay.⁴⁸ For activity assays, *Strep*-Tactin sepharose (IBA, St. Louis, MO) was used to remove contaminating wt-β2 from [NO₂Y₁₂₂]-β2. Typically 4–5 g of cell paste was used. Cell lysis, streptomycin sulfate precipitation, and ammonium sulfate precipitation were carried out as described above. After removal of ammonium sulfate using Sephadex G-25, the desalted protein was loaded onto *Strep*-tactin sepharose column (1 cm × 5 cm, 4 mL), which had been equilibrated in buffer D. The column was washed with buffer D and [NO₂Y₁₂₂]-β2 was eluted with 2.5 mM desthiobiotin in buffer D. Typically, 0.4 mg of [NO₂Y₁₂₂]-β2 per gram of wet cell paste was obtained. The decreased yield is due to a low affinity of [NO₂Y₁₂₂]-β2 for the resin. Protein concentration and iron content were determined as described above.

Generation and Expression of Double Mutants. [NO₂Y₇₃₀]-α2(Y₇₃₁F), [NO₂Y₇₃₀]-α2(Y₇₃₁A), [NO₂Y₇₃₀]-α2(C₄₃₉S), [NO₂Y₇₃₀]-α2(C₄₃₉A), and [NO₂Y₇₃₁]-α2(Y₇₃₀F). Mutations were introduced by PCR as described above with primers in Table S2 in Supporting Information. pBAD-*nrda*-Y₇₃₀Z was used as a template for [NO₂Y₇₃₀]-α2(Y₇₃₁F), [NO₂Y₇₃₀]-α2(Y₇₃₁A), [NO₂Y₇₃₀]-α2(C₄₃₉S), and [NO₂Y₇₃₀]-α2(C₄₃₉A), and pBAD-*nrda*-Y₇₃₁Z was used as a template for [NO₂Y₇₃₁]-α2(Y₇₃₀F). PCR products were amplified in *E. coli* DH5α, and their DNA sequences were confirmed. Expression and purification of these proteins were carried out as described above for [NO₂Y]-α2 single mutants.

Determination of Protein Purity and NO₂Y Incorporation.

The purity of each [NO₂Y]-α2 and [NO₂Y]-β2 was determined from SDS–PAGE and Coomassie staining using Quantity One software (BioRad). The amount of NO₂Y incorporated into α2 or β2 was determined by its phenolate absorption subsequent to its incubation in 6 M guanidine in 50 mM TAPS pH 9.0 at room temperature for 1 h. The measurement was repeated in triplicate. *N*-Acetyl-3-nitrotyrosine amide, prepared as previously described²⁹ and recrystallized from methanol, was used as a standard. The solvent was removed in vacuo over P₂O₅ for 18 h, until no further changes in weight were observed. The extinction coefficient of *N*-acetyl-3-nitrotyrosine amide was determined by weight and UV–vis spectrum.

K_d for the Interaction of β2 and [NO₂Y]-α2s in the Presence of CDP/ATP by Competitive Inhibition Assay.⁴⁹ The assay mixture in a final volume of 300 μL consisted of 0.15 μM β2, 1 mM CDP, 1.6 mM ATP, 50 μM TR, 1 μM TRR, and 0.2 mM NADPH in RNR assay buffer. The reaction was initiated by

adding a mixture of 0.3 μM wt-α2 and variable amounts of [NO₂Y]-α2s (0, 0.1, 0.2, 0.5, 1.0, 2.0, 4.0 μM) and the A_{340 nm} (ε = 6.22 mM⁻¹ cm⁻¹), corresponding to NADPH consumption, was monitored at 25 °C. The data were fit to eq 1:

$$[\text{NO}_2\text{Y}-\alpha 2]_{\text{bound}} = \frac{[\alpha 2\beta 2]_{\text{max}}[\text{NO}_2\text{Y}-\alpha 2]_{\text{free}}}{K_d + [\text{NO}_2\text{Y}-\alpha 2]_{\text{free}}} \quad (1)$$

where [NO₂Y-α2]_{bound} is the concentration of the NO₂Y-α2β2 complex, [α2β2]_{max} is the concentration of the wt-α2β2 complex in the absence of [NO₂Y-α2], and K_d is the dissociation constant of [NO₂Y]-α2 from β2. [α2β2]_{max} was 0.09 μM under these assay conditions. Each data point represents an average of three independent measurements. The K_d for the subunit interaction between α2 and [NO₂Y₁₂₂]-β2 was measured in the identical manner using 0.15 μM wt-α2 and 0.3 μM wt-β2.

Spectrophotometric and Radioactive Activity Assays. The spectrophotometric and radioactive RNR assays were performed as described.²⁹ Typically, [NO₂Y]-α2s (1 or 2 μM), wt-β2 (2, 5, or 10 μM) was incubated with CDP (1 mM), ATP (3 mM) in the presence of TR, TRR, and NADPH in RNR assay buffer. [5-³H]-CDP (5150–5230 cpm/nmol, ViTrax, Placentia, CA) was used in the radioactive assay.

Determination of the pK_a of NO₂Y in [NO₂Y]-α2s and [NO₂Y₃₅₆]-β2 in the Presence of E, E/β2 (or α2), and E/β2(or α2)/S. To determine the pK_a of NO₂Y in the α2 mutants, the absorption spectra from 250 to 700 nm were determined at 25 °C at each pH. Each step in the titration was carried out in a separate cuvette. Good's buffers (50 mM, MES (pH 6.0–6.8), HEPES (pH 7.0–8.0), and TAPS (pH 8.2–9.2) contained 1 mM EDTA and 15 mM MgSO₄. Each buffered solution contained [NO₂Y]-α2 (7.5 μM) and E (ATP or dGTP at 1 and 0.1 mM, respectively), E/β2 (7.5 μM), or E/β2/S (CDP or ADP at 1 mM). The pH was redetermined after mixing all components. To compensate for differences in baseline absorption, all spectra were zeroed at 700 nm. All titrations were conducted in triplicate. Analysis of the titration data was carried out using eq 2:

$$A = \frac{(\epsilon_{\text{H}}K_a[\text{H}^+] + \epsilon^-)[\text{NO}_2\text{Y}-\alpha]}{K_a[\text{H}^+] + 1} \quad (2)$$

where A is the absorbance of the phenolate, ε⁻ is the extinction coefficient of phenolate at its λ_{max}, and ε_H is the extinction coefficient of the phenol at the same wavelength as the phenolate λ_{max}. The data from the plot of A vs pH was fit to eq 2 using Kaleidagraph and nonlinear least-squares curve fitting to determine ε_H, ε⁻ and K_a.

[NO₂Y₃₅₆]-β2, previously prepared by EPL²⁹ was used to determine the pK_a in the complex with α2/ATP/CDP. The titration was carried out as described above, in the presence of E/α2 (1 mM ATP, 7.5 μM α2), or E/α2/S (1 mM CDP). The data were fit to eq 2 to determine the pK_a.

pH Titration of NO₂Y in [NO₂Y₁₂₂]-β2. The absorption spectrum of [NO₂Y₁₂₂]-β2 was determined between pH 7.0 and 10.6 at 25 °C as above. For a pH higher than 9.0, CHES (pH 9.0–10.0) and CAPS (pH 10.3–10.6) were used. Titrations were carried out with [NO₂Y₁₂₂]-β2 (7.5 μM), with [NO₂Y₁₂₂]-β2(7.5 μM)/α2(7.5 μM)/ATP(1 mM)/CDP (1 mM), or with apo-[NO₂Y₁₂₂]-β2 (7.5 μM). The pH was measured after mixing all components. To compensate for differences in baseline absorption, all spectra were zeroed at 700 nm. Apo-[NO₂Y₁₂₂]-β2 was prepared using hydroxyquinoline as a chelator in the presence of 1 M imidazole.⁴¹

Crystallization, Data Collection, and Refinement. Wt-α2 and [NO₂Y]-α2s were co-crystallized with a 20mer peptide⁴ that corresponds to the last 20 amino acids of β2. Crystals were grown for approximately 1 week at 4 °C using the hanging drop vapor diffusion method in EasyXtal Tool plates (QIAGEN). Each drop consisted of 2 μL of α mutant (8–9 mg/mL) and peptide (30 mg/

(48) Fish, W. W. *Methods Enzymol.* **1988**, *158*, 357–364.

(49) Climent, I.; Sjöberg, B.-M.; Huang, C. Y. *Biochemistry* **1991**, *30*, 5164–5171.

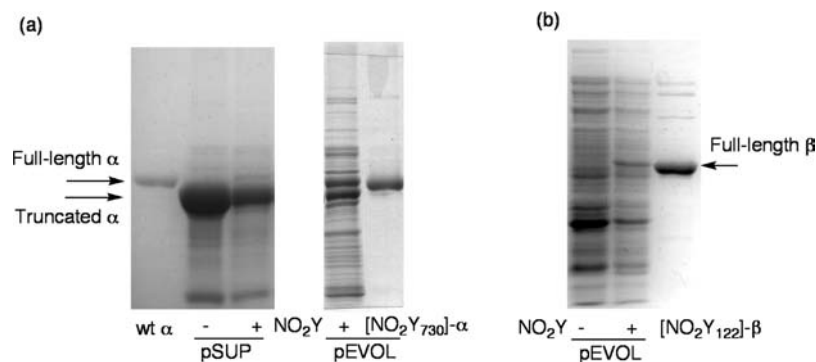


Figure 2. SDS-PAGE of $[\text{NO}_2\text{Y}_{730}]$ - α and $[\text{NO}_2\text{Y}_{122}]$ - β . (a) SDS-PAGE of purified $[\text{NO}_2\text{Y}_{730}]$ - α and whole cell lysate of *E. coli* expressing $[\text{NO}_2\text{Y}_{730}]$ - α using pSUP-3NT/8 (left) and pEVOL- NO_2Y (right). Cells were grown in the presence or absence of NO_2Y as indicated. The position of protein bands for full-length α (85.6 kDa) and truncated α (82.2 kDa) are denoted by arrows. (b) SDS-PAGE of purified $[\text{NO}_2\text{Y}_{122}]$ - β (45.0 kDa) and a whole cell lysate of *E. coli* TOP10/pEVOL- NO_2Y /pBAD-*nrdB*-NS5- Y_{122}Z grown in the absence and presence of NO_2Y as indicated. The truncated protein is 15.9 kDa and thus not observable in this gel (10% acrylamide).

mL) and 2 μL of a solution containing 1.5 M Li_2SO_4 , 2 mM DTT, and 25 mM sodium citrate (pH 6). The crystals were quickly washed in a 1.5 M Li_2SO_4 solution containing 20% ethylene glycol, mounted in fiber loops, and flash-frozen in liquid N_2 .

All sets of data were collected at 100 K at the European Synchrotron Radiation Facility stations (Grenoble, France). The crystals are of the rhombohedral space group R32 with hexagonal axes approximately 225, 225, and 337 Å, containing 3 molecules per asymmetric unit. As a result of the freezing of the crystals, the cells are slightly smaller than the previous data of wt- $\alpha 2$ collected at 4 °C.⁴ Y_{730}F - $\alpha 2$ coordinates⁵ (PDB ID 1R1R) were used as an initial model in refinement of the wt- $\alpha 2$ data (2.3 Å resolution). This wt- $\alpha 2$ structure was then used as a starting model for all $[\text{NO}_2\text{Y}]$ - $\alpha 2$ s. To verify the positions of modifications/mutations, difference maps between the new wt- $\alpha 2$ structure and each $[\text{NO}_2\text{Y}]$ - $\alpha 2$ structure were inspected after the first restrained cycle of refinement. Table S3 in Supporting Information summarizes the details of data collection and refinement.

Results

Incorporation of NO_2Y into $\alpha 2$. The Chin and Mehl groups³⁵ recently reported the evolution of a suppressor tRNA/RS pair for site-specific incorporation of NO_2Y into superoxide dismutase (SOD) expressed in *E. coli*. Initially their construct pSUP-3NT/8, containing the genes for both the tRNA and the RS, was used in combination with pTrc containing *nrdA* (the gene for RNR α) with the TAG codon in place of the tyrosine codon at 730 or 731. pTrc plasmid has recently been successfully used by us to incorporate NH_2Y into the same positions of $\alpha 2$.²³ Expression was carried out in GMLL medium⁴² or in the minimal medium used for NO_2Y incorporation into SOD.³⁵ Under these conditions, however, only very weak expression of truncated $\alpha 2$ was observed. In an effort to enhance expression of α , we cloned *nrdA* into pBAD/*MycHis-A* to generate pBAD-*nrdA* and attempted expression in richer medium.⁵⁰ *E. coli* TOP10 cells were transformed with pSUP-3NT/8 and pBAD-*nrdA*- Y_{730}Z or pBAD-*nrdA*- Y_{731}Z and grown in GMLL medium containing NO_2Y , D-glucose, L-Ara, and 17 proteinogenic amino acids excluding Cys, Tyr, and Phe. Under these conditions, protein expression was robust, giving rise to predominantly truncated α and a small amount of full-length protein (Figure 2a, left gel). Fortunately, most of the truncated protein was insoluble, and thus full-length α was successfully isolated by our standard procedure for α purification that uses a dATP

affinity column,⁴⁶ followed by an additional Q Sepharose column (Figure S1 in Supporting Information). Typically 2.8 mg of $[\text{NO}_2\text{Y}_{730}]$ - $\alpha 2$ and 1.0 mg of $[\text{NO}_2\text{Y}_{731}]$ - $\alpha 2$ per gram of cell paste are isolated. More recently we have used the newly constructed pEVOL- NO_2Y (see below) that results in higher expression levels of full length $[\text{NO}_2\text{Y}_{730(731)}]$ - $\alpha 2$ (Figure 2a, right gel).

The purity of $[\text{NO}_2\text{Y}_{730}]$ - $\alpha 2$ and $[\text{NO}_2\text{Y}_{731}]$ - $\alpha 2$ was determined to be $\sim 95\%$ and $\sim 80\%$, respectively, based on the intensities of the Coomassie stained protein bands on SDS-PAGE gel (Figure S1 and Table S4 in Supporting Information). At pH 9.2, these mutants exhibit a phenolate λ_{max} of 442 and 437 nm, respectively, which is red-shifted 18 and 13 nm from the phenolate λ_{max} of *N*-acetyl-3-nitrotyrosine amide²⁹ (424 nm) in the same buffer (Figure 3a). To calculate the extent of NO_2Y incorporation into α , each $[\text{NO}_2\text{Y}]$ - $\alpha 2$ was denatured in 6 M guanidine HCl in 50 mM TAPS pH 9.2. Both denatured mutants exhibited a phenolate λ_{max} of 435 nm, identical to that of the *N*-acetyl-3-nitrotyrosine amide in the same buffer (Figure S2 in Supporting Information).⁵¹ The extinction coefficient ($\epsilon_{435\text{ nm}}$) of *N*-acetyl-3-nitrotyrosine amide in 6 M guanidine (pH 9.2) was determined to be $4890\text{ M}^{-1}\text{ cm}^{-1}$.⁵¹ By measuring $A_{435\text{ nm}}$ of the denatured $[\text{NO}_2\text{Y}]$ - $\alpha 2$ s, the concentration of NO_2Y in each mutant was determined. These numbers allowed the determination of the purity of $[\text{NO}_2\text{Y}_{730}]$ - $\alpha 2$ and $[\text{NO}_2\text{Y}_{731}]$ - $\alpha 2$ to be $93 \pm 3\%$ and $79 \pm 3\%$, respectively, which correlate well with the purity of $\alpha 2$ determined from SDS-PAGE analysis (Table S4 in Supporting Information), suggesting that the impurity is associated with other proteins and that incorporation of NO_2Y into both $[\text{NO}_2\text{Y}]$ - $\alpha 2$ s is high ($98 \pm 2\%$).

Incorporation of NO_2Y into $\beta 2$. In contrast with the results using pSUP-3NT/8 for the incorporation of NO_2Y into α , efforts to express full-length β with NO_2Y at 122 were unsuccessful, despite detection of substantial amounts of truncated protein. Recently, the Schultz group has developed a new plasmid, pEVOL, in which aminoacyl-RS expression is controlled by the strong L-Ara inducible promoter, *araBAD*.⁴³ pEVOL has been demonstrated to improve suppression relative to other constructs in a number of cases.⁴³ Thus, the NO_2Y -RS was cloned into pEVOL resulting in pEVOL- NO_2Y and used to examine NO_2Y incorporation in place of Y_{122} in $\beta 2$. Successful expression of full-length $\beta 2$ was observed when the protein was

(50) Hammill, J. T.; Miyake-Stoner, S.; Hazen, J. L.; Jackson, J. C.; Mehl, R. A. *Nat. Protoc.* **2007**, *2*, 2601–2607.

(51) The presence of 6 M guanidine HCl perturbed λ_{max} as well as the extinction coefficient of *N*-acetyl-3-nitrotyrosine.

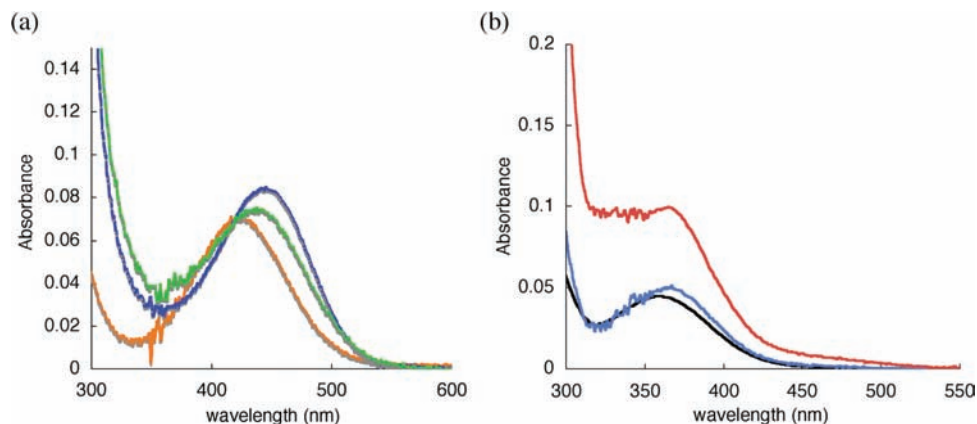


Figure 3. Absorption spectra of nitrophenolate feature of [NO₂Y]-α₂s and nitrophenol feature of [NO₂Y₁₂₂]-β₂. (a) [NO₂Y₇₃₀]-α₂ (blue), [NO₂Y₇₃₁]-α₂ (green), and *N*-acetyl-3-nitrotyrosine amide (yellow) in 50 mM TAPS (pH 9.0), 1 mM EDTA, 15 mM MgSO₄. Spectral intensities were normalized to NO₂Y concentration (15 μM) according to the purity of [NO₂Y₇₃₀]-α₂ (92%), [NO₂Y₇₃₁]-α₂ (79%) determined from A_{435 nm} in 6 M guanidine. (b) Red trace, absorption spectra of [NO₂Y₁₂₂]-β₂ (2.9 Fe/β₂, 15 μM) in HEPPS (pH 7.6); blue trace, absorption spectrum after subtraction of the met-β₂ spectrum (3.2 Fe/β₂, 13.5 μM, the concentration of β₂ was normalized for the iron content); black trace, absorption spectrum of *N*-acetyl-3-nitrotyrosine amide in 50 mM MES (pH 5.0) buffer.

expressed in the amino acid supplemented minimal medium using pEVOL-NO₂Y and pBAD-*nrdB*-NS5-Y₁₂₂Z (Figure 2b). pBAD-*nrdB*-NS5-Y₁₂₂Z encodes β with *Strep*II tag and a 5 amino acid linker (SLGGH) at the N-terminus and a TAG codon (Z) at position 122. We have previously confirmed that the N-terminal *Strep*-tag does not affect the RNR activity.⁴⁷ *Strep*-tagged β₂ will be referred to as β₂. Attempts to purify [NO₂Y₁₂₂]-β₂ with the *Strep*-tactin affinity resin were inefficient as a result of poor binding, yielding 0.4 mg β₂ per gram of cell-paste. Thus, [NO₂Y₁₂₂]-β₂ was purified by our standard procedure for nontagged β₂ using anion exchange column chromatography. Typically 6–7 mg [NO₂Y₁₂₂]-β₂ per gram of cell paste with 90% purity based on SDS–PAGE gel analysis was obtained (Figure 2b, Table S4 in Supporting Information).

As isolated, the absorption spectrum of the purified [NO₂Y₁₂₂]-β₂ showed broad features between 325 and 400 nm and no sharp feature associated with a Y• at 410 nm (Figure 3b). The ferrozine assay revealed 2.9 ± 0.2 Fe/β₂, suggesting that [NO₂Y₁₂₂]-β₂ has a diferric cluster (met form). Thus, if NO₂Y• is formed, it is short-lived. Incorporation of NO₂Y was confirmed to be ~98% as described above for α (Table S4 in Supporting Information). Subtraction of the absorption spectrum of the diferric cofactor cluster (normalized for the iron content) from that of [NO₂Y₁₂₂]-β₂ gave a spectrum with a λ_{max} at 363 nm (ε = 3400 ± 240 M⁻¹ cm⁻¹, Table 1, Figure 3b), consistent with a phenol form of NO₂Y.

Finally, incorporation of NO₂Y in place of Y₃₅₆ was also attempted. Since the truncated β was soluble, C-terminal *strep*-tagged β⁴⁷ was used to facilitate the separation of full-length β from truncated β. The use of pEVOL-NO₂Y and pBAD-NrdB-Y₃₅₆Z resulted in expression of full-length β that was not observed when the protein was expressed in the absence of NO₂Y (Figure S3 in Supporting Information). However, the purified full-length β did not exhibit the phenolate absorption at pH 9.2 under native or denaturing conditions, suggesting the absence of NO₂Y incorporation. An ESI-MS analysis showed the purified β has a molecular mass 15 Da larger than the wt protein (Figure S4 in Supporting Information), which corresponds to an addition of an NH₂ group. No signal corresponding to [NO₂Y₃₅₆]-β₂ was observed. Previous workers have reported that NO₂Y can be reduced to NH₂Y by heme proteins in the

Table 1. Extinction Coefficients of NO₂Y Phenol and Phenolate in RNR

	phenol		phenolate	
	λ _{max} (nm)	ε (M ⁻¹ cm ⁻¹) ^b	λ _{max} (nm)	ε (M ⁻¹ cm ⁻¹) ^a
<i>N</i> -Ac-NO ₂ Y-NH ₂	360	2960	424	4610
[NO ₂ Y ₇₃₀]-α ₂	360	3800 ± 170	442	6400 ± 250
[NO ₂ Y ₇₃₁]-α ₂	360	4200 ± 300	437	5200 ± 300
[NO ₂ Y ₇₃₀]-α ₂ (Y ₇₃₁ F)	360	3400 ± 160	445	6200 ± 210
[NO ₂ Y ₇₃₀]-α ₂ (Y ₇₃₁ A)	360	4100 ± 200	435	7000 ± 200
[NO ₂ Y ₇₃₀]-α ₂ (C ₄₃₅ S)	360	3700 ± 220	442	6800 ± 240
[NO ₂ Y ₇₃₀]-α ₂ (C ₄₃₅ A)	360	3400 ± 230	442	6000 ± 220
[NO ₂ Y ₇₃₁]-α ₂ (Y ₇₃₀ F)	360	4000 ± 230	437	5900 ± 150
[NO ₂ Y ₁₂₂]-β ₂ (met form)	363	3400 ± 240 ^c	nd	nd
[NO ₂ Y ₁₂₂]-β ₂ (apo form)	363	3400 ± 240	425	4200 ± 220

^a Extinction coefficients of phenolates were determined from pH titration curve fitting to eq 2. The titration curves were generated by plotting absorbance at indicated phenolate λ_{max} as a function of pH. Titration curves used are shown in Figure 5 and Figure S7 in Supporting Information. ^b Extinction coefficients of phenol were calculated from the UV–vis spectrum at pH 6.0. ^c The extinction coefficients of [NO₂Y₁₂₂]-β₂ (met form) was determined from the absorption spectrum at pH 7.6 after subtracting a spectrum of wt met-β₂ normalized by the iron content.

presence of thiols or ascorbic acid.⁵² Since residue 356 is surface exposed, it is likely to have been reduced in *E. coli* cells.

Determination of the K_d for Subunit Interactions. The K_d for subunit interactions in wt-RNR is weak [0.06–0.2 μM in the presence of CDP and ATP,⁴⁹ (A. Q. Hassan and J. Stubbe, unpublished results) and 0.4 μM in the absence of nucleotides⁵⁴]. Perturbation of subunit interactions by NO₂Y incorporation was thus a concern as 731 is thought to reside at the subunit interface. Thus, the K_d was determined by the procedure of Climent et al.,⁴⁹ using the [NO₂Y]-α₂s and [NO₂Y₁₂₂]-β₂ as a competitive inhibitor of wt-α₂ and -β₂ interactions. This method gave a K_d of 1.32 ± 0.10 μM, 0.51 ± 0.07 μM, and 0.40 ± 0.06 μM for [NO₂Y₇₃₀]-α₂, [NO₂Y₇₃₁]-α₂, and [NO₂Y₁₂₂]-β₂, respectively (Table 2). Since the formation of the phenolate of NO₂Y could

(52) Balabanli, B.; Kamisaki, Y.; Martin, E.; Murad, F. *Proc. Natl. Acad. Sci. U.S.A.* **1999**, *96*, 13136–13141.

(53) Baldwin, J.; Krebs, C.; Ley, B. A.; Edmondson, D. E.; Huynh, B. H.; Bollinger, J. M. *J. Am. Chem. Soc.* **2000**, *122*, 12195–12206.

(54) Hassan, A. Q.; Wang, Y.; Plate, L.; Stubbe, J. *Biochemistry* **2008**, *47*, 13046–13055.

Table 2. K_d of [NO₂Y]- α 2s with wt- β 2 or [NO₂Y₁₂₂]- β 2 with wt- α 2

	K_d (μ M) ^a
[NO ₂ Y ₇₃₀]- α 2	1.32 \pm 0.10
[NO ₂ Y ₇₃₁]- α 2	0.51 \pm 0.07
[NO ₂ Y ₇₃₀]- α 2(Y ₇₃₁ F)	1.45 \pm 0.14
[NO ₂ Y ₇₃₀]- α 2(Y ₇₃₁ A)	2.71 \pm 0.13
[NO ₂ Y ₇₃₀]- α 2(C ₄₃₉ S)	1.28 \pm 0.07
[NO ₂ Y ₇₃₀]- α 2(C ₄₃₉ A)	2.07 \pm 0.07
[NO ₂ Y ₇₃₁]- α 2(Y ₇₃₀ F)	0.50 \pm 0.04
[NO ₂ Y ₁₂₂]- β 2	0.40 \pm 0.06

^a K_d was determined at pH 7.6 by using [NO₂Y]- α 2s or [NO₂Y₁₂₂]- β 2 as competitive inhibitors of CDP reduction by α 2, β 2, TR, TRR, and NADPH.⁴⁹

Table 3. RNR Activities of [NO₂Y]- α 2s and [NO₂Y₁₂₂]- β 2

	radioactive RNR assay (% wt) ^a	spectrophotometric RNR assay (% wt) ^a	yield (mg/g)
[NO ₂ Y ₇₃₀]- α 2	1.1	1.5	2.8
His-[NO ₂ Y ₇₃₀]- α 2 ^{b,c}	0.5	0.5	5.8
[NO ₂ Y ₇₃₁]- α 2	2.9	3.1	1
[NO ₂ Y ₇₃₁]- α 2 ^b	0.6	0.4	2.4
[NO ₂ Y ₇₃₀]- α 2(Y ₇₃₁ F)	2.5	2.7	0.8
[NO ₂ Y ₇₃₀]- α 2(Y ₇₃₁ A)	1.8	2.0	1.4
[NO ₂ Y ₇₃₀]- α 2(C ₄₃₉ S)	2.4	2.6	1.1
[NO ₂ Y ₇₃₀]- α 2(C ₄₃₉ A)	2.7	2.8	0.8
[NO ₂ Y ₇₃₁]- α 2(Y ₇₃₀ F)	1.7	1.3	2
[NO ₂ Y ₁₂₂]- β 2 ^{b,d}	0.39	0.29	7
[NO ₂ Y ₁₂₂]- β 2 ^{b,e}	>0.01	>0.1	0.4

^a Activities are reported as % activity of wt- α 2 (2500 nmol/min/mg) or wt- β 2 (6500 nmol/min/mg). ^b Expressed using pEVOL-NO₂Y. ^c His-tagged NrdA purified with Ni-NTA column chromatography. See Materials and Methods for detail. ^d Purified using DEAE and Q-sepharose. ^e Purified using strep-Tactin sepharose.

perturb subunit interactions, the K_d was also determined at pH 6.8 where the phenol is completely protonated. The observed K_d for [NO₂Y₇₃₁]- α 2 (0.53 \pm 0.07 μ M) is essentially the same as that at pH 7.6. In general, the interactions are weaker than those observed in wt RNR. Unexpectedly, the K_d of [NO₂Y₇₃₀]- α 2 is higher than that of [NO₂Y₇₃₁]- α 2, even though Y₇₃₁- α 2 is closer to the subunit interface.⁴ This knowledge facilitated design of studies, pK_a determination and activity assays, where the subunits need to be associated.⁵⁵

Catalytic Activity of [NO₂Y]- α 2s: Levels of Endogenous wt- α . The genes for RNR are essential, and therefore expression of [NO₂Y]- β or [NO₂Y]- α mutants in *E. coli* is accompanied by expression of small amounts of the endogenous wt subunit. The purification protocol for [NO₂Y₃₅₆]- β 2 made by EPL ensured the removal of wt- β and thus a lower limit of detection of deoxynucleotide formation for this mutant of <1/10⁴ that of wt- β 2 was set.²⁹ The absence of activity was expected on the basis of the experimentally measured differences in peak potentials of the NO₂Y and Y of 210 mV (pH 7.6)²⁹ and our previous studies with F_nY ($n = 2-4$) at the same position, which suggested that when the F_nY was more difficult to oxidize than Y by 200 mV, RNR was inactive.²⁰

Activity of [NO₂Y₁₂₂]- β 2, purified by conventional anion exchange chromatography methods or by affinity chromatography, was determined. In the former case, the [NO₂Y₁₂₂]- β 2 had activity 1/250 and in the latter case <1/10⁴ that of the wt- β 2 (Table 3). Thus, [NO₂Y₁₂₂]- β 2 is inactive.

The activity assays of [NO₂Y₇₃₀]- and [NO₂Y₇₃₁]- α 2, Table 3, revealed activity levels of 0.5–1.5% for [NO₂Y₇₃₀]- α 2 (1/

Table 4. pK_a of [NO₂Y₇₃₀]- α 2 and Related Double Mutants^a

	[NO ₂ Y ₇₃₀]- α 2	[NO ₂ Y ₇₃₀]- α 2 (Y ₇₃₁ F)	[NO ₂ Y ₇₃₀]- α 2 (C ₄₃₉ S)	[NO ₂ Y ₇₃₀]- α 2 (C ₄₃₉ A)	[NO ₂ Y ₇₃₀]- α 2 (Y ₇₃₁ A)
ATP	7.9	7.9	8.3	8.3	6.5
ATP/ β 2	7.9	7.9	8.4	8.3	6.6
ATP/ β 2/CDP	8.3	8.2	8.3	8.5	7.0
dGTP	7.8	7.9	8.4	8.3	6.5
dGTP/ β 2	7.8	7.9	8.5	8.4	6.5
dGTP/ β 2/ADP	8.2	8.2	8.4	8.6	6.8

^a pK_a s were determined by fitting eq 2 to the pH titration curve generated by plotting phenolate absorption intensities as a function of pH. Measurements were carried out in the presence of E, E/ β 2 and E/ β 2/S and performed in triplicate. Errors were \pm 0.05 pH units.

200 to 1/100) to 0.4–2.9% for [NO₂Y₇₃₁]- α 2 (1/250 to 1/30) that of wt- α 2. Three arguments support our conclusion that the observed activity is predominantly associated with endogenous wt- α . First, there is a rough correlation between the levels of expression of the mutants and their activity (Table 3): the higher the yield of the mutant protein, the lower the activity. Expression of [NO₂Y₇₃₁]- α , for example, with two different suppression constructs gives rise to activity that varies 5-fold. Second, a number of double mutants, described below, with NO₂Y and a block (Phe) in the ET pathway, all have activities in the range of 1–3% (1/30 to 1/100) that of wt. The Phe mutants themselves have been deemed inactive with similar levels of activity.¹³ Third, the activity measured for [NO₂Y]- α 2 assayed at 2 μ M is independent of the concentration of β 2 (2, 5, or 10 μ M) used in the assay mixture. Based on the K_d for subunit interactions, the RNR activity would have been expected to increase with the increasing concentrations of β 2 as a result of increased α β 2 complex formation.⁵⁵

Finally, we have recently developed an affinity chromatography method to remove endogenous levels of wt- α 2 from [NH₂Y]- α 2s by constructing an N-terminally tagged α , into which the unnatural amino acid is incorporated (E. C. Minnihan, and J. Stubbe, unpublished results). Use of this construct to generate [NO₂Y₇₃₀]- α 2 gave protein of 92% purity and activity 0.5% that of wt- α 2 at pH 7.6. The activity is also 0.50 \pm 0.02% that of wt- α at pH 6.5 and 8.6. If the mechanism of oxidation of C₄₃₉ involves hydrogen atom transfer, then at pH 8.6 the relative activity should be reduced to <25% of that at pH 6.8, as the NO₂Y is predominantly the phenolate at pH 8.6 (see titration data below and Table 4). From the arguments presented above we have assumed that all of the [NO₂Y]- α 2s and β 2s are inactive and that the detected activity is associated with endogenous wt- α or with the infidelity of the RS associated with mischarging the tRNA with Y.

Determination of the pK_a s of [NO₂Y]- α 2s. The ability to form [NO₂Y]- α 2 β 2 complexes incapable of turnover has enabled us to determine the pK_a of NO₂Y at positions 730 and 731 in α 2 in the presence of S (ADP or CDP) and S/E pair (CDP/ATP or ADP/dGTP). As noted above, S and E are critical as they trigger the active conformation for PCET. The pH measurements of the α 2 β 2 complex were performed between pH 6.0–9.2 with [NO₂Y]- α 2 and β 2 in which 65% of [NO₂Y₇₃₀]- α 2 and 77% of [NO₂Y₇₃₁]- α 2 are in a complex based on the K_d (Table 2). An additional experiment was carried out with 92% complex formation with similar results. The errors in the pK_a values were \pm 0.05 pH units. The protein stability was also ascertained at the two pH extremes (6.0 and 9.2) by incubating the wt RNR at these pHs for 15 min followed by an activity assay at pH 7.6. In each case 95% of the activity was retained. The results of a typical pH titration in the presence of E are shown in Figure

(55) Ge, J.; Yu, G.; Ator, M. A.; Stubbe, J. *Biochemistry* **2003**, *42*, 10071–10083.

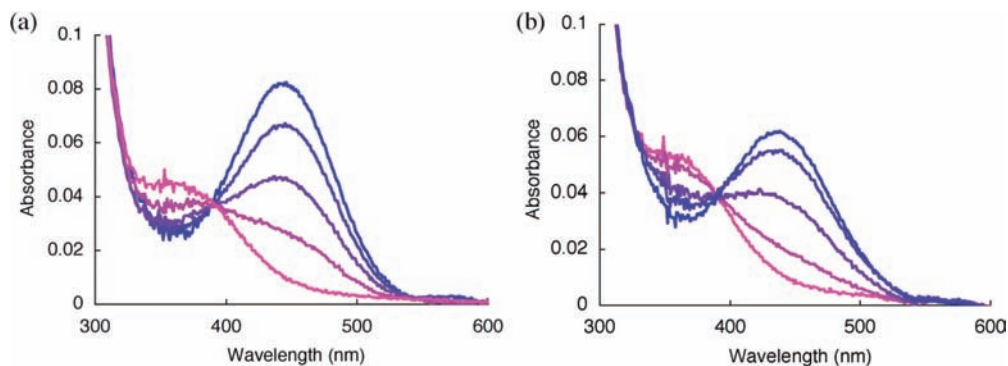


Figure 4. UV-vis absorption spectra of (a) [NO₂Y₇₃₀]-α2 (7.5 μM) and (b) [NO₂Y₇₃₁]-α2 (7.5 μM) at pH 6.0 (pink trace), 7.4, 8.0, 8.6, and 9.2 (blue trace) in the presence of 1 mM ATP. Loss of the phenol feature (360 nm) occurs concomitantly with the formation of the phenolate feature (442 and 437 nm for [NO₂Y₇₃₀]-α2 and [NO₂Y₇₃₁]-α2, respectively) with increasing pH (pink to blue).

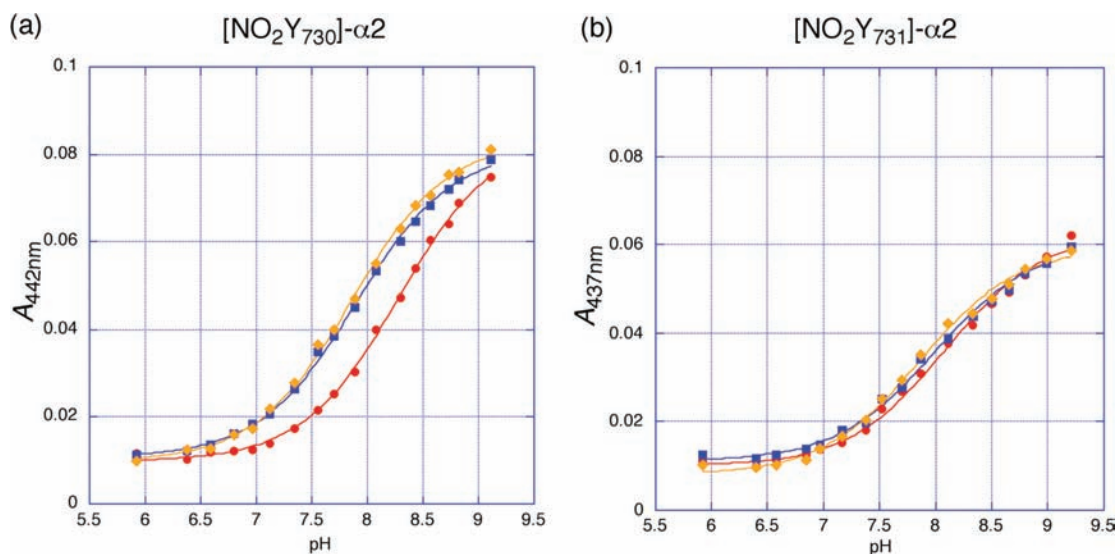


Figure 5. Titration curves of (a) [NO₂Y₇₃₀]-α2 and (b) [NO₂Y₇₃₁]-α2 in the presence of 1 mM ATP (yellow diamonds), 1 mM ATP and 7.5 μM β2 (blue squares) and 1 mM ATP, 7.5 μM β2 and 1 mM CDP (red circles). Absorption at 442 and 437 nm was monitored for [NO₂Y₇₃₀]-α2 and [NO₂Y₇₃₁]-α2, respectively. Each data point represents an average of three replicates. Lines are from fits to eq 2.

Table 5. pK_a of [NO₂Y₇₃₁]-α2 and [NO₂Y₇₃₁]-α2(Y₇₃₀F)^a

	[NO ₂ Y ₇₃₁]-α2	[NO ₂ Y ₇₃₁]-α2 (Y ₇₃₀ F)	[NO ₂ Y ₇₃₁]-α2/Y ₃₅₆ F-β2
ATP	7.9	7.4	
ATP/β2	8.0	7.4	7.8
ATP/β2/CDP	8.0	7.7	7.8
dGTP	7.9	7.4	
dGTP/β2	8.0	7.5	7.9
dGTP/β2/ADP	7.9	7.7	7.9

^a pK_as were determined as described in the footnote of Table 4. Titrations were carried out in the presence of E, E/β2 and E/β2/S and performed in triplicate. Errors were ±0.05 pH units.

4. As the pH increases, the absorption of the phenol decreases concomitant with an increase in the absorption of the phenolate with an isosbestic point at 393 nm. Plots of the intensity of the phenolate absorption versus pH are shown in Figure 5. The data is best fit to eq 2²⁹ for a species undergoing a single deprotonation. The pK_as of NO₂Y in each [NO₂Y]-α2 are summarized in Tables 4 and 5 and can be compared to the pK_a 7.1 for NO₂Y in the C-terminal 20mer peptide of β2.²⁹ The pK_a of [NO₂Y₇₃₀]-α2 with E is 7.9 and 7.8 for ATP and dGTP, respectively. These pK_as remain unchanged upon addition of β2. Addition of S to the [NO₂Y₇₃₀]-α2/E/β2 complex, either a purine or a pyrimidine, increased the pK_a by 0.4 pH units. The

pK_a of NO₂Y at 731 is similar to 730 when titrated with E or E/β2; however, no further change is observed on S addition.

The extinction coefficients for the phenolate of each NO₂Y in α2 were also determined by fits to eq 2 and are 6400 ± 250 and 5200 ± 300 M⁻¹ cm⁻¹ for [NO₂Y₇₃₀]-α2 and [NO₂Y₇₃₁]-α2, respectively (Table 1). These values are larger than those determined for *N*-acetyl-3-nitrotyrosine amide under the same conditions (λ_{max} 424 nm, ε_{424 nm} 4610 M⁻¹ cm⁻¹). The extinction coefficients of phenols were also calculated from the absorbance at λ_{max} at pH 6.0 (Table 1). The differences in extinction coefficients and shifts in λ_{max} of the mutants are reporting on their surrounding environment but are difficult to interpret. To obtain insights about the effects of surrounding environment, the absorption spectra of *N*-acetyl-3-nitrotyrosine amide were determined in various organic solvents with 1% triethylamine (Figure S5, Table S5 in Supporting Information). Red-shifted phenolate absorptions (440–458 nm) were observed in nonprotic polar solvents (DMSO, DMF and acetonitrile). In contrast, in protic solvents (water, ethanol, and methanol), the phenolate absorbs at shorter wavelength, 418–424 nm. Thus, the red shifts of NO₂Y observed at 731 and 730 may suggest a less protic environment. π–π stacking interactions and NO₂ group orientation, however, can also affect the phenolate absorption,

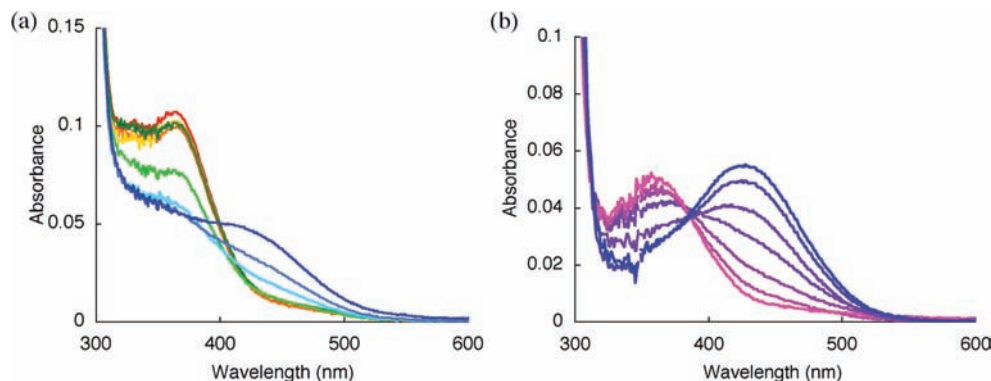


Figure 6. UV-vis absorption spectra of (a) met-[NO₂Y₁₂₂]-β₂ at pH 7.1 (red), 7.6 (orange), 8.2 (yellow), 8.6 (dark green), 9.0 (light green), 9.2 (light blue), 9.5 (blue) and 10.0 (dark blue), and (b) apo-[NO₂Y₁₂₂]-β₂ at pH 7.6 (pink trace), 8.4, 9.0, 9.6, 10.0, 10.3, and 10.6 (blue trace).

and theoretical studies using structures described below are ongoing to better understand the environment of each Y.

pH Titration of [NO₂Y]-β₂. The pH titration of [NO₂Y₁₂₂]-β₂ was carried out between pH 7.0 and 10.0 (Figure 6a) with the spectra from pH 7.6–8.6 being identical. At pH 9.0, a decrease in A_{360 nm} is observed without a corresponding increase in the region of the phenolate, 420–450 nm. At pH > 9.2, further decrease in absorption in the 320–360 nm region occurs along with an increase in the phenolate region, although no isosbestic point is apparent. The unusual absorption spectra at pH values greater than 9 for [NO₂Y₁₂₂]-β₂ may be due to the decomposition of the diferric cluster that generates apo-β₂, which then allows titration of NO₂Y₁₂₂. Quantitation of iron in [NO₂Y₁₂₂]-β₂ at pH 10.0, for example, showed complete iron loss (Table S6 in Supporting Information) and the phenolate absorption observed is close to that predicted from the pK_a of this residue in apo-β₂ (see below). Thus, the pK_a of the iron loaded form (met form) cannot be directly determined. Since the spectra between pH 7.6–8.6 are identical, and 10% of phenolate would result in a detectable change in absorbance (0.007, assuming an ε = 4200 M⁻¹ cm⁻¹), a lower limit of detection of the pK_a of the phenol can be set at 9.6. The pK_a perturbation of NO₂Y₁₂₂ is thus greater than 2.5 pH units. Results from the titration of [NO₂Y₁₂₂]-β₂ with wt-α₂/E/S are similar to the titration without α₂ (Figure S6 in Supporting Information).

In contrast, a pH titration of NO₂Y was successfully carried out between pH 7.0–10.6 with apo-[NO₂Y₁₂₂]-β₂, which does exhibit an isosbestic point (Figure 6b). Titration above pH 10.8 was not possible due to protein precipitation. These data, fit to eq 2, gave a pK_a of 9.8. This pK_a is close to the lower limit of pK_a for the met form (9.6), indicating that the diferric cluster does not significantly lower the phenol pK_a. The λ_{max} and the extinction coefficient of phenolate were minimally perturbed from that of *N*-acetyl-3-nitrotyrosine amide in water (Table 1).

The pK_a of [NO₂Y₃₅₆]-β₂ was also revisited using ATP/CDP. [NO₂Y₃₅₆]-β₂ prepared by EPL²⁹ was used because of the reduction of NO₂Y in 356 of β₂ incorporated by the orthogonal tRNA/RS methodology. The pK_a with ATP/α₂ and ATP/α₂/CDP are very similar to the previously determined pK_a with dGTP/α₂/ADP (Table 6). For all of the NO₂Y mutants, ATP/CDP and dGTP/ADP gave almost identical pK_as.

pK_as of [NO₂Y]-α₂s with a Second Mutation Adjacent to NO₂Y in the PCET Pathway. The crystal structure of GDP/TTP bound *E. coli* α₂ indicates that the distance between the oxygens of the phenol of Y₇₃₁ and Y₇₃₀-α₂ is 3.3 Å and the distance between the oxygen of Y₇₃₀-α₂ and the sulfur of C₄₃₉-α₂ is 3.4 Å.⁵ The distances indicate the possibility of H-bonding

Table 6. pK_a of [NO₂Y₃₅₆]-β₂^a

	[NO ₂ Y ₃₅₆]-β ₂
α, α ₂ ^c	7.1 ^b
ATP/α ₂	7.2 ^b
ATP/α ₂ /CDP	7.5
dGTP/α ₂ /ADP	7.3 ^b

^a [NO₂Y₃₅₆]-β₂ was prepared by EPL and its pK_as were determined as described previously.²⁹ Titrations were carried out in the presence of E/α₂ and E/α₂/S and performed in triplicate. Errors were ±0.05 pH units. ^b Values reported previously.²⁹ ^c α is in equilibrium between monomer and dimer without nucleotides.⁴⁰

interactions between these species, which likely plays an important role in PCET.^{56–59} The structure also suggests an unusual π–π stacking interaction of Y₇₃₁- and Y₇₃₀-α₂, which may also be of interest mechanistically, although the degree of stacking varies in recent structures of α from other sources.^{60,61} Removal of a H-bonding interaction or the π stacking might perturb the pK_a of the phenolic hydroxyl group. A variety of double mutants (Y to Phe/Ala and Cys to Ser/Ala) were successfully expressed and isolated. Their purity was similar to the corresponding parent single mutant (Table S4 in Supporting Information).

The λ_{max} and ε of the phenolate and the K_d for subunit interactions for each double mutant were determined (Tables 1 and 2) and are similar to those of the parent single mutant. Conservative substitutions minimally perturbed the K_d, while the nonconservative substitution of Ala for C₄₃₉ or Y₇₃₁ in [NO₂Y₇₃₀]-α₂ resulted in large K_d perturbations (Table 2). As noted above, all double mutants showed specific activities of 1–3% of wt-α₂, similar to the single mutants and presumably associated with endogenous wt-α₂.

The pK_a of each double mutant was determined (Tables 4 and 5, Figure S7 in Supporting Information). With [NO₂Y₇₃₀]-α₂, Y₇₃₁ was replaced with Phe and C₄₃₉ with Ala, mutations that disrupt the putative H-bonding. C₄₃₉ was also replaced with

(56) Sjödin, M.; Irebo, T.; Utas, J. E.; Lind, J.; Merényi, G.; Åkermark, B.; Hammarström, L. *J. Am. Chem. Soc.* **2006**, *128*, 13076–13083.

(57) Skone, J. H.; Soudackov, A. V.; Hammes-Schiffer, S. *J. Am. Chem. Soc.* **2006**, *128*, 16655–16663.

(58) Ludlow, M. K.; Skone, J. H.; Hammes-Schiffer, S. *J. Phys. Chem. B.* **2008**, *112*, 336–343.

(59) Mayer, J. M.; Hrovat, D. A.; Thomas, J. L.; Borden, W. T. *J. Am. Chem. Soc.* **2002**, *124*, 11142–11147.

(60) Xu, H.; Faber, C.; Uchiki, T.; Fairman, J. W.; Racca, J.; Dealwis, C. *Proc. Natl. Acad. Sci. U.S.A.* **2006**, *103*, 4022–4027.

(61) Uppsten, M.; Färnegårdh, M.; Jordan, A.; Eliasson, R.; Eklund, H.; Uhlin, U. *J. Mol. Biol.* **2003**, *330*, 87–97.

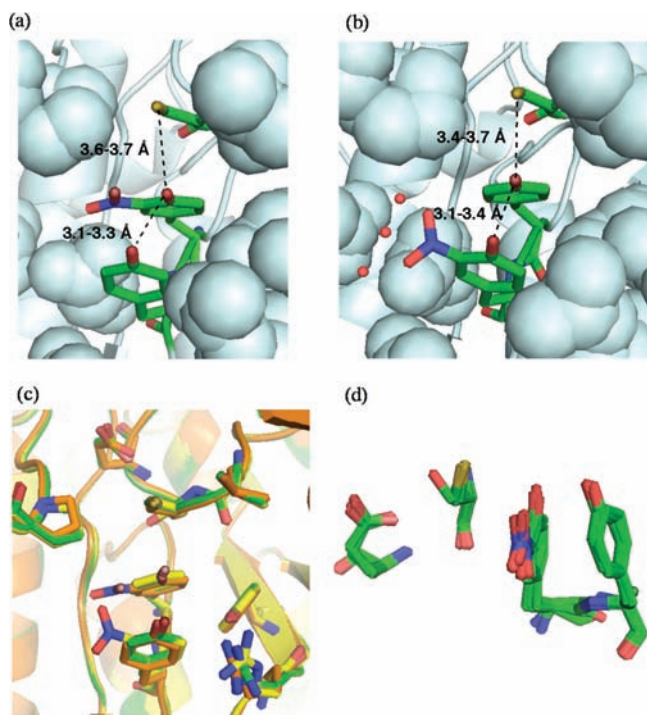


Figure 7. Crystal structures of the radical propagation pathway in [NO₂Y]-α2 mutants. The crystals were grown at pH 6.0–6.5. Oxygens are colored in red, nitrogens in blue, and sulfurs in gold. Pathway residues 731, 730, and 439 are shown with sticks. In the structure of (a) [NO₂Y₇₃₀]-α2 and (b) [NO₂Y₇₃₁]-α2, the dotted lines indicate the distances between the phenolic oxygens and the phenolic oxygen of the 730 residue and the sulfur of C₄₃₉ with distance variations associated with the three subunits in the asymmetric unit. The surrounding residues are shown as spheres. (c) An overlay of the structures of wt-α2 (green), [NO₂Y₇₃₀]-α2 (orange), and [NO₂Y₇₃₁]-α2 (yellow), generated using PyMOL 1.1 (DeLano Scientific LLC) software. Other residues shown are P₆₂₁, E₄₄₁, L₄₃₈, Y₄₁₃ and R₄₁₁. (d) An overlay of the structures of [NO₂Y₇₃₀]-α2 and the double mutants C₄₃₉S, C₄₃₉A, Y₇₃₁A, and Y₇₃₁F. Residues shown are (from the left) 441, 439, 730, and 731.

Ser that could enhance H-bonding. With the C₄₃₉A double mutant, the pK_a was increased from 7.9 to 8.3/8.4 in the presence of E (ATP or dGTP) or E/β2 and addition of S (CDP or ADP) again perturbed the pK_a by 0.2 to 0.3 units. With Y₇₃₁F, the addition of S also elevated the pK_a to 8.2. Only in the case of C₄₃₉S did addition of substrate appear to have no effect. However, as will be seen from the structures described in the following section, [NO₂Y₇₃₀]-α2/C₄₃₉S is the only mutant in which 439 is H-bonded to the active site E₄₄₁ (Figure 7d). Thus, we propose that S binding would disrupt this H-bonding interaction and reset the pK_a to 7.9, while S binding would then perturb the pK_a to 8.3 as observed with the other mutants. These studies reveal that S binding generally elevates the pK_a of residue 730 and that this increase is independent of H-bonding ability of the residues at 439 and 731.

Studies with [NO₂Y₇₃₀]-α2 and Y₇₃₁ replaced with an Ala were also examined to address the putative importance of π–π stacking interactions. The perturbations in pK_a for this mutant were the largest observed in any of the titrations, decreasing from 7.8/7.9 (single mutant) to 6.5 (double mutant) in the presence of E. The observed pK_as are 0.6 units lower than that of the *N*-acetyl-3-nitrotyrosine amide. However, even in this case, the pK_a was substantially increased, from 6.5 to 6.8/7.0, on addition of S. This double mutant also exhibited the largest perturbation in K_d (Table 2), suggesting that the structure of the complex is perturbed by this nonconservative substitution.

Titration studies were also carried out with [NO₂Y₇₃₁]-α2 and Y₃₅₆F-β2 and with the double mutant where Y₇₃₀ was replaced with F. In the former case, the pK_a was unaffected by S addition. However, the pK_a of the Y₇₃₀F double mutant decreased 0.5 units relative to the single mutant with E and E/wt-β2 and increased back toward that of the single mutant pK_a on addition of S. The studies in sum suggest that S perturbs the pK_a at 730 with minimal effect at 731 and that the altered pK_as do not appear to be the result of increased H-bonding by residues adjacent to the substitution.

Crystal Structures of [NO₂Y]-α2s. Understanding the experimental data obtained with the unnatural amino acid probes in α and β requires structural information and computational efforts. As a first step toward structural characterization, crystals of wt and seven [NO₂Y]-α2 mutants were obtained in the presence of a 20mer peptide, identical to the C-terminal 20 amino acids of β, using crystallization conditions similar to those previously reported for wt-α2.⁴ The structure of wt-α2, isolated by methods similar to the [NO₂Y]-α2, was solved by molecular replacement using Y₇₃₀F-α2 (PDB ID 1R1R).⁵ This new wt-α2 structure (2.3 Å resolution) was then used as the starting point to solve the [NO₂Y]-α2 structures, which were obtained and refined to 2.1–3.1 Å resolution. In all mutants, there are three α subunits in the asymmetric unit with two of the three subunits forming a dimer. The data collection methods and refinement statistics are summarized in Table S3 in Supporting Information. In general, the structures revealed minimal overall perturbation relative to the wt structure and the phenyl rings and OH groups of NO₂Ys superimposed well with the corresponding residues in the wt structure (Figure 7). In all of the structures the distances between the oxygens of the two phenols (at 731 and 730) and of the phenol and the thiol (at 730 and 439) are very similar to the distances found in wt-α and are within H-bonding distance in the former case and slightly longer than H-bonding distance in the latter case.

The NO₂ group in all of the structures lies on the sterically less crowded side, the left side looking toward C₄₃₉ from Y₇₃₁ (Figure 7a and 7b). At 730, the NO₂ group in all single and double mutants lies in the plane of the phenyl ring. No additional electron density is apparent in the vicinity of [NO₂Y₇₃₀]-α2 that can be associated with water. On the other hand, the NO₂ group at 731 has different orientations in each of the three αs in the asymmetric unit. In two of the αs, the NO₂ group is perpendicular to the plane of the phenyl ring, while in the remaining α, it is almost parallel to the ring. The oxygens of the NO₂ group have H-bonding interactions with H₂O(s), which are distinct within each α. The double mutant (Y₇₃₀F) also has its NO₂ group perpendicular to the phenyl ring, but no waters are identifiable.

Finally a superposition of all of the [NO₂Y₇₃₀]-α structures (Figure 7D) shows that residue 439 adopts a different conformation in the serine mutant, in which the OH of serine appears to H-bond to E₄₄₁, a key residue in the active site involved in catalysis. The SH of Cys in the wt-α2, on the other hand, points toward residue 730. Thus, the structures in general suggest H-bonding interactions are important in the PCET with C₄₃₉ showing the greatest flexibility. The detailed analysis of the structures is ongoing and will be published subsequently. Ultimately, structures with S, E, and β2 bound will be critical

to understanding the role of H-bonding interactions in the radical propagation process.

Discussion

Understanding of the radical propagation process in RNR requires an understanding of factors that control the different mechanisms of PCET in well-defined model systems where the rate constants for oxidation can be measured and the parameters that influence these rate constants such as H-bonding, electronic effects, and the proton acceptor can be manipulated.^{56,58,62–67} Different types of models will be required to probe PCET within β and within α of RNR (Figure 1). Hydrogen-bonded phenols, for example, have been designed to understand the oxidation of the Y_Z in photosystem II in which a histidine functions as the proton acceptor from Y_Z during its oxidation.^{68,69} Phenols with amine and imidazole bases^{62,63,70} and carboxylates^{56,65,66} appended *ortho* to the phenol have been synthesized and structurally and spectroscopically characterized. The rate constants for oxidation and the deuterium kinetic isotope effects on oxidation have been measured as a function of temperature.^{56,62,65,66,70} The Hammarström model seems particularly appropriate for Y_{356} oxidation in RNR where E_{350} is proposed to be the initial proton acceptor (Figure 1). However, appropriate models for the putative H-bond network between $Y_{731}/Y_{730}/C_{439}$, with no obvious base proximal to either Y, are not yet available.

As a starting point to understanding the PCET in RNR, we have chosen NO_2Y and NH_2Y as reporters on the H-bonding interactions of each Y in the ground states and the transient $Y\bullet$ intermediate states in the radical propagation process, respectively. In the former case, we proposed that the phenol pK_a might be altered by the protein environment on binding of the second subunit and/or S/E. In the latter case, 1H and 2H ENDOR spectroscopy might allow direct observation of H-bond interactions to the radical intermediates.⁷¹ The focus of this paper is NO_2Y .

To carry out these studies, the evolved tRNA/RS method pioneered by the Schultz lab⁴² was optimized to site-specifically incorporate high levels of NO_2Y in place of Y_{122} , Y_{731} , and Y_{730} . Our efforts to insert NO_2Y in place of Y_{356} have thus far been unsuccessful due to reduction during the expression process. The inactivity of these mutants has allowed us to determine the pK_a of each NO_2Y in the $\alpha 2\beta 2$ complex in the presence of substrate (S) and effector (E), presumably in the “active” conformation required for PCET. Together with our previous pK_a data for $[NO_2Y_{356}]\beta 2$, the results presented show the power of site-specific incorporation of unnatural amino acids to

measure individual pK_a s in a protein with 1135 amino acids. These measurements for four different NO_2Y s, provide an important step in understanding radical initiation in RNR.

Mechanistic Insights. Our pH titration data has established that each Y in the pathway (Figure 1) has distinct properties. The greatest pK_a perturbations are observed with $NO_2Y_{122}\beta 2$: elevations of 2.7 and >2.5 units in the apo and met form, respectively. This Y is unique in that its oxidation results in a stable $Y\bullet$ ($t_{1/2}$ of 4 days at 4 °C) and it is generated by the metal cluster. An explanation for its unusual stability is clear from a comparison of X-ray crystal structures of met- $\beta 2^6$ ($\beta 2$ with $Y\bullet$ reduced-diferric cluster), apo- $\beta 2$,⁷² and $Mn_2\beta 2$ ⁷³ and results from single crystal high field EPR spectroscopy of the active diferric- $Y\bullet\beta 2$.⁷ In the crystal structure of the class Ia $Mn_2\beta 2$ ⁷³ the $Y_{122}\text{-OH}$ is within H-bonding distance to D_{84} , a carboxylate ligand to Mn1 (corresponds to Fe1 in Figure 1b) of the cluster, that in turn may H-bond with a H_xO ($x = 1, 2$) bound to the same Mn (Figure 1b). If similar interactions exist in the diferric cluster during radical propagation in the presence of $\alpha/S/E$, then the close interaction of the phenol with the D_{84} carboxylate would preclude its ionization, to prevent electrostatic repulsion with D_{84} . The pK_a of 9.8 for NO_2Y in apo- $[NO_2Y_{122}]\beta 2$ suggests that its environment, even in the apo form, is very hydrophobic (Q_{80} , I_{231} , I_{234} , F_{208} , L_{77} , F_{212} , Figure S8 in Supporting Information). On the other hand, high field EPR spectroscopy of active $\beta 2$ ($Y\bullet$) reveals that this Y_{122} is no longer H-bonded.⁷ Our current model is that only subsequent to S/E binding in α is PCET initiated and the $Y\bullet$ reoriented toward D_{84} so that it can pick up a proton from the H_2O bound to Fe1 concomitant with its reduction by W_{48} .^{12,14,15} Thus, the environment of the $Y\bullet$ is such that it is stable, unless a proton is also available. The elevated pK_a of NO_2Y observed in our titrations is consistent with concerted PCET mechanism for Y_{122} oxidation in which the proton donor is distinct from the reductant (W_{48}).

The pK_a s of NO_2Y at 356 in $\beta 2$ and 730 and 731 in $\alpha 2$ are perturbed to a much smaller extent than at 122 with perturbations increasing as the distance of the Y increases from Y_{122} (7.5,⁷⁴ 7.9, and 8.3 for NO_2Y 356, 731, and 730, respectively). The perturbation ranges from 0.4 to 1.2 units relative to NO_2Y within the 20mer C-terminal peptide. These measurements demonstrate that Nature has evolved a different type of environment for transient radical formation and a different mechanism for their oxidation. The pK_a at each transient $Y\bullet$ site is discussed.

Studies in a variety of enzymes containing redox cofactors have established that binding of substrate provides a mechanism to perturb the reduction potential of the cofactor and to facilitate the chemistry.^{75,76} We thus investigated whether the addition of the correct S/E pair to RNR could alter the pK_a of each Y and provide insight about its oxidation mechanism. The pK_a of NO_2Y_{730} is uniquely increased by 0.4 units on addition of either a purine or pyrimidine substrate to the $[NO_2Y_{730}]\alpha 2/\beta 2/E$. The basis for this perturbation and the potential importance of the H-bond network was investigated by titration studies with double mutants that have altered H-bonding capabilities in residues adjacent to $NO_2Y_{730}\alpha 2$. The parallel NO_2 group orientation

(62) Markle, T. F.; Rhile, I. J.; DiPasquale, A. G.; Mayer, J. M. *Proc. Natl. Acad. Sci. U.S.A.* **2008**, *105*, 8185–8190.

(63) Rhile, I. J.; Markle, T. F.; Nagao, H.; DiPasquale, A. G.; Lam, O. P.; Lockwood, M. A.; Rotter, K.; Mayer, J. M. *J. Am. Chem. Soc.* **2006**, *128*, 6075–6088.

(64) Mayer, J. M. *Annu. Rev. Phys. Chem.* **2004**, *55*, 363–390.

(65) Johannissen, L. O.; Irebo, T.; Sjödin, M.; Johansson, O.; Hammarström, L. *J. Phys. Chem. B.* **2009**, *113*, 16214–16225.

(66) Irebo, T.; Johansson, O.; Hammarström, L. *J. Am. Chem. Soc.* **2008**, *130*, 9194–9195.

(67) Hammes-Schiffer, S.; Soudackov, A. V. *J. Phys. Chem. B* **2008**, *112*, 14108–14123.

(68) Lomoth, R.; Magnuson, A.; Sjödin, M.; Huang, P.; Styring, S.; Hammarström, L. *Photosynth. Res.* **2006**, *87*, 25–40.

(69) Mayer, J. M.; Rhile, I. J.; Larsen, F. B.; Mader, E. A.; Markle, T. F.; DiPasquale, A. G. *Photosynth. Res.* **2006**, *87*, 3–20.

(70) Markle, T. F.; Mayer, J. M. *Angew. Chem., Int. Ed.* **2008**, *47*, 738–740.

(71) Seyedsayamdost, M. R.; Argirević, T.; Minnihan, E. C.; Stubbe, J.; Bennati, M. *J. Am. Chem. Soc.* **2009**, *131*, 15729–15738.

(72) Aberg, A.; Nordlund, P.; Eklund, H. *Nature* **1993**, *361*, 276–278.

(73) Högbom, M.; Andersson, M. E.; Nordlund, P. *J. Biol. Inorg. Chem.* **2001**, *6*, 315–323.

(74) pK_a of $NO_2Y_{356}\beta 2$ was determined using the mutant prepared by EPL, which requires two additional mutations, V353G and S354C, that reduce the activity to 25% that of the wt activity.

(75) Sliagar, S. G.; Gunsalus, I. C. *Proc. Natl. Acad. Sci. U.S.A.* **1976**, *73*, 1078–1082.

(76) Stankovich, M. T.; Soltysik, S. *Biochemistry* **1987**, *26*, 2627–2632.

relative to the plane of the phenyl group with all mutants suggests that relative pK_as are informative. In all cases except C₄₃₉S, addition of substrate elevates the pK_a regardless of the H-bonding interactions, consistent with an increased hydrophobic environment. No waters are identifiable in the region surrounding 730. The observations with the Ser mutant can also be rationalized as described in the Results. At present, we do not know if this small perturbation is mechanistically important or why the pK_a is increased. Finally, it is also likely that if H-bonding is key to the mechanism of the thiyl radical generation, it may be manifested predominantly in the transition states of the reaction and may not be readily apparent from this type of ground-state analysis.^{15,65}

The two remaining Ys (Figure 1) are located at the subunit interface, and unfortunately no structural information is available for the active $\alpha 2\beta 2$ complex. Our studies, however, with 3,5-F₂Y at Y₃₅₆ revealed that nucleotide reduction can occur through the phenolate form of this residue, consistent with nonobligate coupling of the electron and proton transfer and with the proton transfer occurring orthogonal to the ET pathway.²¹ The minimal perturbation of the NO₂Y pK_a at this position suggests it may be more solvent exposed in the complex than Y₇₃₀, which is also consistent with our recent studies using an environmentally sensitive fluorophore attached at 356.⁵⁴ Our current hypothesis for PCET at this position is that orthogonal PCET occurs with transfer of a proton to E₃₅₀ within the C-terminal tail of β . The importance of this residue in nucleotide reduction was demonstrated by previous studies of Climent et al.¹⁶ with a E₃₅₀A mutant and our recent studies with a E₃₅₀Q mutant (unpublished results). As noted above, the model studies of Hammarström may thus provide a model of PCET at this center.^{56,66}

The pK_a of NO₂Y₇₃₁ and its minimal perturbation in double mutants with Y₃₅₆F and Y₇₃₀F suggests that H-bonding is again not observable at this position and that this residue may be solvent-exposed. The structure of the single mutant shows that the NO₂ group is more flexible at this position with conformations both parallel and perpendicular to the plane of the phenyl ring and that it H-bonds with specific water molecules that are distinct in each α . Sequence analysis of conserved residues of RNR with the constraint that they reside within the subunit interface based on the docking model⁴ reveal only E₃₅₀ and R₂₃₆ in β and no interesting conserved residues in α . Studies on R₂₆₅ mutants in mouse β , corresponding to the R₂₃₆ mutant in *E. coli* β , have been interpreted to support a role for this residue in the proton coupling in the propagation pathway.⁷⁷ However, since the R₂₆₅E mutant exhibited 40% the activity of the wt

enzyme, it is unlikely to function as a proton acceptor. Unfortunately, interactions that are proposed to be important in our models for radical propagation in RNR (Figure 1)^{14,15} are not apparent from the pK_a measurements. Our studies suggest that the pK_as of the Ys that undergo transient oxidations during radical propagation in RNR do not appear to be significantly perturbed. Computational efforts are underway to use the structural information to understand the pK_a perturbations.

Summary

Despite the prevalence of PCET in biological systems, pK_a information of individual redox-active residues in proteins is scarce. A general method for directly measuring the pK_a of a single residue within a protein would be mechanistically useful.⁷⁸ In this paper NO₂Y has been used as a probe to measure the pK_a perturbations of all redox-active Ys, 122- and 356⁷⁴- $\beta 2$, 731- and 730- $\alpha 2$, in the radical propagation pathway in *E. coli* RNR. The crystal structures of the [NO₂Y]- $\alpha 2$ mutants have shown minimal structural perturbations. The pH titrations have shown position-dependent pK_a perturbations at these redox-active Y sites with the largest and distinct perturbation at the stable tyrosyl radical site, Y₁₂₂- $\beta 2$. The study reveals distinct environments for the stable and transient Y•. The pK_a information reported is essential to understand the mechanism of long-range PCET in RNR.

Acknowledgment. We thank Ellen C. Minnihan for helpful discussions. This work was supported by the NIH grant GM29595 to J.S.

Supporting Information Available: SDS–PAGE of purified [NO₂Y]- α s; absorption spectra of [NO₂Y]- $\alpha 2$ s in their denatured state; absorption spectra of *N*-acetyl-3-nitrotyrosine amide (0.2 mM) in organic solvent; SDS–PAGE and ESI-QTOF-MS of β expressed in *E. coli* TOP10/pBAD-NrdB-CS(Y356Z)/pEVOL-NO₂Y; UV–vis absorption spectra of [NO₂Y₁₂₂]- $\beta 2$ with $\alpha 2$ /ATP/CDP; pH titration curves of [NO₂Y]- $\alpha 2$ s; the environment of Y₁₂₂ in the crystal structure of wt- $\beta 2$; pK_as of *o*-, *m*-, and *p*-nitrophenol in solution; primers used for cloning and site-directed mutagenesis; crystallographic data collection and refinement statistics; the purity of [NO₂Y]- $\alpha 2$ s and $\beta 2$; λ_{\max} of *N*-acetyl-3-nitrotyrosine in organic solvent with 1% triethylamine; stability of diferric cluster of met-[NO₂Y₁₂₂]- $\beta 2$ in basic conditions. This material is available free of charge via the Internet at <http://pubs.acs.org>.

JA101097P

(77) Nárvaez, A. J.; Voevodskaya, N.; Thelander, L.; Gräslund, A. *J. Biol. Chem.* **2006**, *281*, 26022–26028.

(78) Hay, S.; Westerlund, K.; Tommos, C. *Biochemistry* **2005**, *44*, 11891–11902.